Algerian Democratic and Popular Republic
Ministry of Higher Education and Scientific Research
KASDI MERBAH UNIVERSITY OUARGLA
Faculty of New Information and Communication Technologies
Department of Computer Science and Information Technology

Thesis Submitted in Candidacy for a Master Degree in computer science, option

Artificial Intelligence and Data Science

by Belbey Sara Rayhane & Mehammedi Khadidja

Wildfire Final Burned Area Estimation Using Enhanced U-Net Architectures: New Deep Learning Approachs

Jury Members:

Dr.	zerdoumi Oussama	Jury Chair	UKM Ouargla
Dr.	Khadra Bouanane	Supervisor	UKM Ouargla
Dr.	Said Bachir	CO Supervisor	UKM Ouargla
Dr.	Khaldi Belal	Reviewer	UKM Ouargla

Academic year: 2023/2024

Dedication

In reaching this significant academic milestone, I offer sincere dedication to those whose influence has been pivotal to my journey.

*Foremost to myself, thanks to **Allah**, this achievement reflects my resilience, determination, and unwavering commitment to my ambitions. I extend my gratitude for the countless hours of hard work, for persisting through obstacles, and for consistently striving for excellence. I recognize my dedication to ongoing growth, which has propelled my academic achievements. I embrace my passion and expertise in my field, fueling the perseverance poured into this thesis. While I set high standards for myself, I acknowledge the dedication and effort that have led me to this point.*

To my parents, whose unwavering support and belief in my potential have fueled my ambition and guided me to this milestone. I am deeply grateful for your sacrifices and constant presence.

To my siblings and aunt, their understanding and support have been invaluable.

In appreciation of Khadidja for her hard work and commitment, her contributions have been crucial to our project.

Sara Rayhane

First and foremost, I want to express my gratitude to Allah. I sincerely want to appreciate Allah for giving me the courage, guidance, and direction I needed to successfully complete my thesis. This success would not have been achieved without His guidance and permission.

To my parents, I am truly grateful for their financial and emotional support. I have achieved so much in this educational journey due to the fact that they have always believed in me and constantly supported me. I am grateful for the sacrifices they made for me

I express my deepest gratitude to my siblings for their support. Their encouragement has been a constant source of motivation throughout this journey.

I would like to thank my colleague Rayhane for her hard work and dedication. I am thankful for the friendship and teamwork that enabled us to successfully complete our theses.

To myself, I am grateful for the perseverance, commitment, and resilience demonstrated throughout my academic journey. Despite facing numerous obstacles, I have persevered, reaching significant milestones and accomplishments. This journey has been one of profound personal development, brimming with invaluable insights and growth. I am grateful for the strength and perseverance that have brought me to this point, and I eagerly anticipate continuing to strive for excellence in all future endeavors.

Khadidja

ABSTRACT

Wildfires are a significant environmental and economic threat, requiring advanced methods for accurate prediction and damage assessment. Deep learning has demonstrated remarkable capabilities in many fields, including wildfire management, primarily due to its ability to automate and improve prediction processes. Previous research has shown limitations due to the complexity of the phenomenon and nature of the data.

In this thesis, we present our contributions to enhancing wildfire final burned area prediction through the integration of deep learning techniques, specifically U-Net architectures.
We conducted a comparative study to evaluate different U-Net architectures, including the standard U-Net, U-Net++, and Dense U-Net, on the Mesogeos Final Burned Area Prediction dataset. The Dense U-Net outperformed others, demonstrating its robustness in handling complex wildfire data. Subsequently, Dense U-Net was used to create two enhanced models. The first model improved Dense U-Net using a regularization approach, providing detailed burned area estimations, while the second model incorporated a refinement module to improve the accuracy of burned area segmentation. Both models showed significant improvements over previous studies. Our research explored various challenges, including data complexity and imbalance, contributing to the development of more effective tools for wildfire management.

KEYWORDS

Wildfire management, Final Burned Area Prediction, U-Net architectures, Dense U-Net, Data Imbalance, Mesogeos Dataset

ملخص

الحرائق البرية تمثل تهديدًا بيئيًا واقتصاديًا كبيرًا، مما يتطلب وسائل متقدمة للتنبؤ الدقيق وتقييم الأضرار. أظهرت تقنيات التعلم العميق قدرات ملحوظة في مجالات عديدة، بما في ذلك إدارة الحرائق البرية، بفضل قدرتها على أتمتة وتحسين عمليات التنبؤ. أظهرت الأبحاث السابقة قيوداً ناتجة عن تعقيد الظاهرة وطبيعة

في هذه الأُطروحة، نقدم إسهاماتنا في تعزيز التنبؤ بمساحة الأراضي المحترقة النهائية للحرائق البرية من البيانات. خلال دمج تقنيات التعلم العميق، وتحديداً هندسة U-Net .

قمنا بدراسة مقارنة لتقييم مختلف هندسات U-Net ، بما في ذلك U-Net ، و U-Net++ ، و Dense U-Net ، على مجموعة بيانات توقعات مساحة الأراضي المحترقة النهائية من Mesogeos . أظهرت Dense U-Net أداءً أفضل من الآخرين، مما يدل على قدرتها على التعامل مع بيانات الحرائق البرية المعقدة بشكل فعال. بعد ذلك، استخدمت Dense U-Net لإنشاء نموذجين محسنين. النموذج الأول قام بتحسين Dense U-Net باستخدام Regularization ، مما يوفر تقديرات مفصلة لمناطق الأراضي المحترقة، بينما قام النموذج الثاني بدمج وحدة تكرير لتحسين دقة تقسيم مناطق الأراضي المحترقة. أظهر كلا النموذجين تحسينات كبيرة على الدراسات السابقة. استكشفت بحوثنا تحديات مختلفة، بما في ذلك تعقيد البيانات وعدم التوازن، مساهمة في تطوير

الكلمات المفتاحية: إدارة الحرائق البرية، توقعات مساحة الأراضي أدوات أكثر فعالية لإدارة الحرائق البرية. المحترقة النهائية، هندسات U-Net ، Dense U-Net ، عدم التوازن في البيانات، Mesogeos Dataset

RÉSUMÉ

Les incendies de forêt représentent une menace environnementale et économique significative, nécessitant des méthodes avancées pour la prédiction précise et l'évaluation des dommages.
L'apprentissage profond a démontré des capacités remarquables dans de nombreux domaines, y compris la gestion des incendies de forêt, principalement en raison de sa capacité à automatiser et améliorer les processus de prédiction. Les recherches antérieures ont montré des limites en raison de la complexité du phénomène et de la nature des données.

Dans cette thèse, nous présentons nos contributions à l'amélioration de la prédiction de la superficie finale brûlée des incendies de forêt grâce à l'intégration de techniques d'apprentissage profond, en particulier les architectures U-Net.

Nous avons mené une étude comparative pour évaluer différentes architectures U-Net, y compris U-Net standard, U-Net++, et Dense U-Net, sur l'ensemble de données de prédiction de la superficie finale brûlée Mesogeos. Dense U-Net a surpassé les autres, démontrant sa robustesse dans le traitement des données complexes des incendies de forêt. Par la suite, Dense U-Net a été utilisé pour créer deux modèles améliorés. Le premier modèle a amélioré Dense U-Net en utilisant une approche de régularisation, fournissant des estimations détaillées de la superficie brûlée, tandis que le deuxième modèle a incorporé un module de raffinement pour améliorer la précision de la segmentation de la superficie brûlée. Les deux modèles ont montré des améliorations significatives par rapport aux études précédentes. Nos recherches ont exploré divers défis, y compris la complexité des données et le déséquilibre, contribuant au développement d'outils plus efficaces pour la gestion des incendies de forêt.

MOTS-CLÉS:

Gestion des incendies de forêt, Prédiction de la superficie brûlée finale, Architectures U-Net, Dense U-Net, Déséquilibre des données, Mesogeos Dataset

Contents

List of Figures

General Introduction

Wildfires are a natural, devastating phenomenon that is uncontrolled. It occurs in natural landscapes and poses significant threats to both humans and ecosystems [7]. Wildfires have become a major environmental challenge due to their increasing frequency and intensity. This increase is influenced by a complex interplay of meteorological, ecological, and human factors [8]. Climate change, urbanization, and land management practices have significantly changed natural fire patterns, especially in vulnerable regions like the Mediterranean [9]. Wildfires' substantial risks to human life, infrastructure, and ecosystem services make them one of the most pressing global threats [10–12], there is a critical need for effective prediction and monitoring technologies. In response to these challenges, advancements in technology, particularly in the fields of remote sensing and artificial intelligence, offer promising solutions where traditional methods of wildfire monitoring and prediction have been supplemented by advanced machine learning and deep learning, significantly enhancing our ability to detect and manage wildfires more effectively [13].

Predicting the extent of wildfires is crucial for several reasons, including protecting the environment and minimizing economic damage. However, previous studies have faced several issues that limit the accuracy and performance of wildfire prediction models, include neglecting external factors like weather conditions and vegetation, as well as problems with data availability and quality due to the complexity of the phenomena, they also struggle with generalizability across regions.

Wildfire datasets commonly exhibit imbalances between burned and non-burned areas, complicating model training and leading to biased predictions Therefore achieving high accuracy in predicting wildfire extent and behavior remains a persistent challenge.

To address these challenges and limitations, this thesis aims to contribute to the field of wildfire management by developing robust methods to predict the extent of wildfire utilizing advanced deep learning techniques, specifically the U-Net [4] and its variants, for wildfire burned area prediction

and estimation, Our study also aims to enhance model generalizability across different regions, and increase prediction accuracy. Our main contributions are summarized as follows:

- We conducted literature review on the use of machine learning and deep learning techniques for wildfire prediction and management, providing insights into current state-of-the-art methods.
- We performed a comprehensive comparative study of three different models: U-Net, U-Net++, and Dense U-Net, to identify the most effective model for predicting final burned areas.
- We developed an approach integrating Dense U-Net for wildfire segmentation and burned area estimation, enhancing the Dense U-Net architecture for improved performance.
- We presented an advanced architecture, designed to improve the accuracy and reliability of wildfire predictions, and conducted thorough evaluations of its performance compared to previous models.

Our thesis is organized as follows:

Chapter 1: In this chapter, we introduce the problem of wildfires, providing an in-depth look into the nature of wildfires, their causes (factors influencing them), and their consequences (impacts). We cover the significance of understanding wildfires, emphasizing the importance of wildfire prediction and management. A comprehensive literature review on the applications of machine learning and deep learning in this domain is presented.

Chapter 2: In this chapter, we explore the methodologies and significance of predicting the burned area and the size of wildfires. The chapter also reviews relevant literature and existing approaches to these prediction tasks.

Chapter 3: In the third chapter, we focus on a comparative study of three different models: U-net, U-net++, and dense U-net. We provide details on the dataset used (Mesogeos), the methodologies applied, and the performance metrics evaluated. This comparative analysis aims to identify the most effective model for predicting final burned in the Mediterranean region.

Chapter 4: In this chapter, we present a novel approach integrating dense U-net for the tasks of wildfire segmentation and burned area estimation. We discuss the enhancements made to the dense U-net architecture and evaluate its performance against other models.

Chapter 5: In this chapter, we present an advanced Denoising Dense U-Net architecture, designed to improve the accuracy and reliability of wildfire predictions. We describe the architecture, implementation, and evaluation of its performance in comparison to previous models.

CHAPTER 1

INTRODUCTION TO WILDFIRE PHENOMENON

1 INTRODUCTION

Wildfires are uncontrolled fires that can arise within natural landscapes, including forests, grasslands, and various other ecosystems. They can burn both on the ground and within the vegetation above, such as tree canopies [7]. wildfires play indispensable roles in shaping terrestrial ecosystems and influencing the carbon cycle by disrupting and rejuvenating ecological processes [14].

Wildfires pose significant risks to human populations, infrastructure, and ecosystem services, particularly in areas where wildlands meet urban development. Human activities, along with climate change, have disrupted natural fire regimes, especially in regions like the Mediterranean [9]. In recent times, wildfires have emerged as one of the most pressing global challenges, leading to substantial loss of life, economic devastation, and environmental deterioration. The frequency and intensity of wildfires have surged, compounded by factors such as climate change, urbanization, and land management practices.

2 THE MULTIFACETED IMPACT OF WILDFIRES: ECOLOGICAL, HEALTH, SOCIOECONOMIC, AND CLIMATE CONSEQUENCES

Wildfires represent a complex and multi-dimensional threat, affecting ecosystems, human health, economies, and climate dynamics. Their consequences extend far beyond ecological and environmental spheres, with profound impacts on public health, socioeconomic stability, and global climate patterns. Understanding the diverse and interconnected effects of wildfires is essential for developing effective mitigation and adaptation strategies to address this growing challenge.

2.1 ECOLOGICAL AND ENVIRONMENTAL IMPACT

Devastating effects on wildlife include injuries and fatalities. Animals can suffer burns on their faces and limbs, with some experiencing deep burns on the skin. The extent, depth, and location of burns must be carefully assessed in affected animals [10].

(a) Evia, Greece - August 8, 2021. *Giorgos Moutafis* [1]

(b) Wildfire aftermath in Varibobi area Aug 5,2021.[2]

(c) Achallam villagers battling wildfires. Tizi Ouzou, Algiers - Aug 18, 2021. [3]

(d) Tizi Ouzou facing wildfire threats. Algiers - Aug 18, 2021.[4]

Figure 1.1: Photographs illustrate the impacts of wildfires in Greece and Algeria

Aquatic fauna are also significantly impacted by wildfires, especially in bodies of water where they may seek refuge [10]. High temperatures during wildfires can exceed lethal limits for water, causing heat damage. Changes in pH, turbidity, the accumulation of toxins, and sedimentation can harm aquatic animals.

Soil and ecosystem dynamics are altered post-wildfire, affecting habitat and food availability for wildlife [10]. Increased light, temperature, and wind lead to changes in soil processes and vegetation structure. Loss of coverage exposes small species to predators, impacting wildlife distribution.

[1]Source for a: https://www.instagram.com/p/CSV840_qyXz

[2]Source for b: https://media.npr.org/assets/img/2021/08/13/ap21217518733715_custom-23980e243bc71841d0bbfae728ec87979a23c9e1.jpg

[3]Source for c and d: https://www.thenationalnews.com/mena/2021/08/18/as-wildfires-dampen-misinformation-threatens-more-lives-in-algeria/

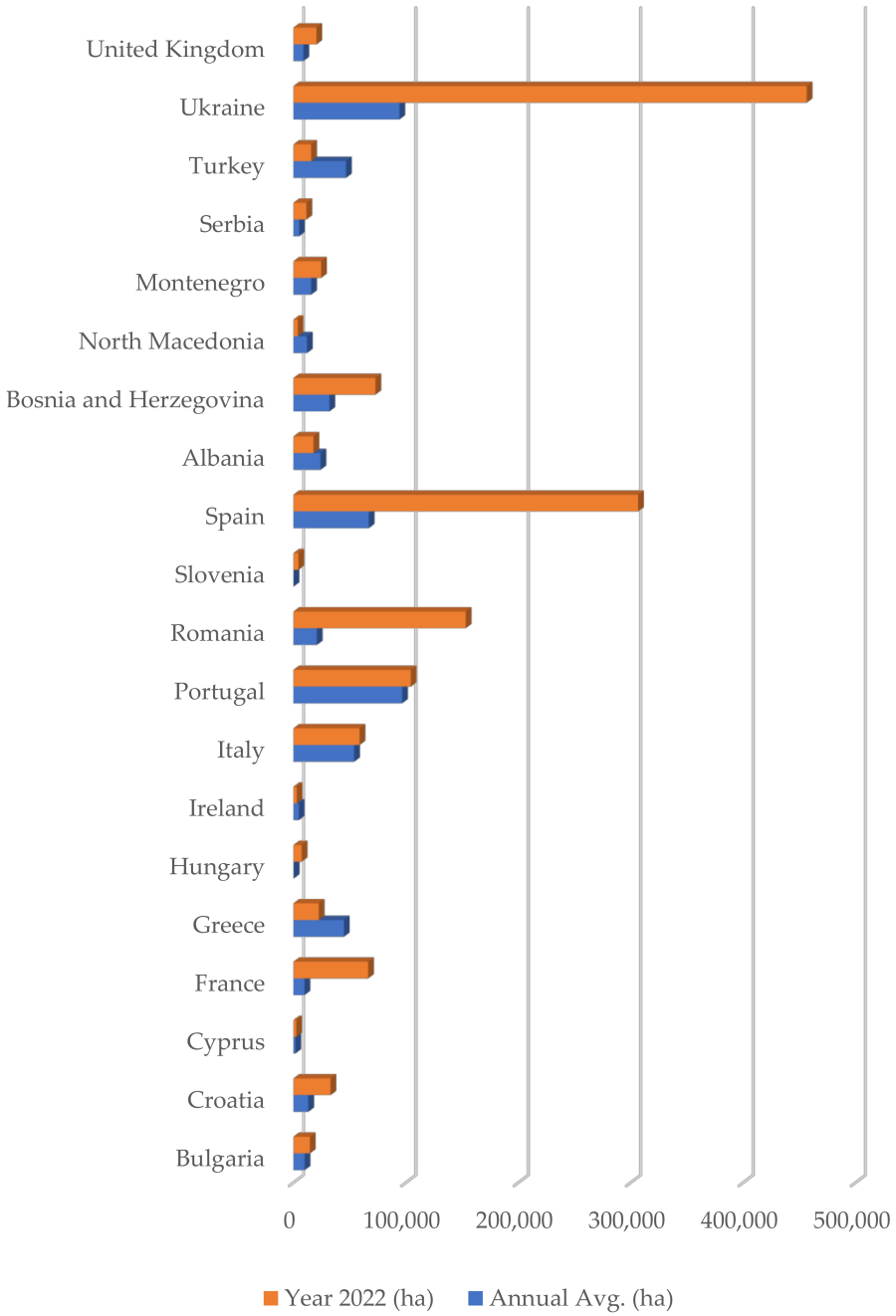

Figure 1.2: Area Affected by Forest Fires in European Countries, Data from the EFFIS—European Forest Fire Information System (2023) [1].

2.2 HEALTH IMPACT

Wildfires are a significant source of air pollution, exacerbating cardiorespiratory diseases like asthma, especially in pediatric populations. There is an increase in asthma exacerbations during wildfire smoke events, with a notable incidence rate ratio in children with asthma. Poor air quality from wildfires is linked to an increased risk of asthma requiring emergency department visits. Wildfires contribute to global air pollution, increasing morbidity and mortality, this is demonstrated by the extensive wildfires witnessed in Canada alone, where over 1.8 million hectares were engulfed by flames in 2019. emphasizing the scale of the issue and its health implications [12].

2.3 SOCIOECONOMIC IMPACT

Economic damage, loss of life, and threats to biodiversity, cultural resources, and property. Evidenced by events like the 2018 Camp Fire in California, resulting in loss of lives, displacement, and billions of dollars in damages [15]. Millions of acres have already been burned, and numerous communities are at risk each wildfire season.

2.4 CLIMATE DYNAMICS

The emission of significant amounts of carbon dioxide and aerosols is contributing to global carbon emissions and altering regional climate patterns. Health impacts due to wildfire smoke, including respiratory and cardiovascular illnesses, pose significant public health challenges [11]. Threatening biodiversity, cultural resources, and property.

3 FACTORS INFLUENCING WILDFIRES

Wildfires are complex phenomena influenced by various factors operating at different spatial and temporal scales that interact to determine their occurrence, behavior, and impact on ecosystems and human communities. Understanding these factors is crucial for effective wildfire management and mitigation strategies [8].

3.1 METEOROLOGICAL FACTORS

Meteorological conditions, including wind speed, air temperature, and soil moisture, play pivotal roles in shaping the spread and intensity of wildfires. In regions like NSW (New South Wales),

Australia, where wildfires are prevalent, these factors have been identified as key drivers of fire behavior [8].

TEMPERATURE

High temperatures can increase the likelihood of wildfires by drying out vegetation and making it more susceptible to ignition. The rate at which a wildfire's temperature rises or falls can have a big influence on the fire's behavior and severity. Reduced temperatures can decrease the rate of spread, while higher temperatures might dry up vegetation and make it more prone to igniting. As such, successful wildfire prediction and management depend heavily on the monitoring of temperature variations.

HUMIDITY

It is often expressed as a percentage and represents the amount of water vapor in the atmosphere. Temperature, weather patterns, and geographic location are a few factors that might influence humidity levels. Humidity conditions have a significant impact on wildfire behavior, and they also play a role in determining fire speed and severity.

PRECIPITATION

Insufficient rainfall can lead to dry conditions, promoting the spread of wildfires.

WIND SPEED AND DIRECTION

The rate of air movement around a fire during a wildfire is referred to as its wind speed, Wind can rapidly spread fires, affecting their direction and intensity. Accelerated wind speeds have the potential to accelerate the spread of wildfires by delivering embers and flames that can exacerbate the fire and ignite additional regions.

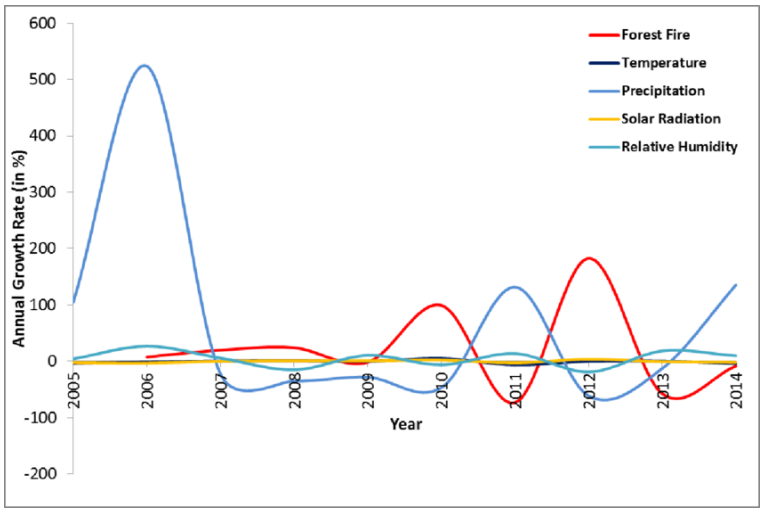

Figure 1.3: Analysis of Increment Rate across meteorological variables versus forest fire events [2].

3.2 VEGETATION

The type and density of vegetation are important indicators of wildfire susceptibility. Changes in vegetation cover and health can influence the likelihood and severity of wildfires, affecting ecosystem resilience and recovery [8].

The Normalized Difference Vegetation Index (NDVI) is a remote sensing metric that quantifies vegetation health and density. Calculated using a specific formula, NDVI values range from -1 to +1, with higher values indicating healthy vegetation and lower values suggesting stressed or sparse vegetation [16].

The type of vegetation in an area can greatly affect the spread and intensity of wildfires. Different types of plants burn at varying rates and temperatures, impacting the overall behavior of a fire. Additionally, the density and moisture content of vegetation can also play a role in how quickly a fire spreads.

3.3 HUMAN ACTIVITY

Human activity can also strongly contribute to the growth and spread of wildfires. Intentional burning of forests, throwing of cigarettes or other burning materials, and improper disposal of flammable materials can all lead to an increased risk of wildfires. It is important for individuals to be aware of their actions and take caution to prevent unintentional fires from starting [8].

POPULATION DENSITY

Areas with higher population densities are more prone to human-caused wildfires due to increased human activities, such as campfires, discarded cigarettes, or equipment use, which can ignite fires.

Human settlements in densely populated areas can lead to the encroachment of residential areas into wildland-urban interfaces, where human infrastructure interfaces with natural vegetation, increasing the likelihood of fire ignitions.

LAND USE CHANGES

Alterations in land use patterns, such as deforestation, urbanization, or agricultural expansion, can modify vegetation cover and fuel loads, potentially increasing fire risk. Changes in land use can lead to the fragmentation of natural habitats, altering ecosystem dynamics, and creating conditions conducive to the rapid spread of fires.

4 CHALLENGES IN COMBATING WILDFIRES

Fighting wildfires poses terrible challenges, characterized by their unpredictability and the dynamic nature of the environment in which they occur.

Factors such as rapid urbanization, climate change-induced weather patterns, and the complex interplay of vegetation, fuel, and wind make traditional resource allocation strategies inadequate and insufficient [17].

5 NEED FOR PREDICTION TECHNOLOGIES

The increasing frequency and severity of wildfires, particularly in regions like the United States and Mediterranean countries, underscore the urgent need for advanced prediction technologies. Climate change and anthropogenic activities have exacerbated these trends, leading to catastrophic events with profound impacts on the economy, human health, ecosystems, and the built environment.

Real-time monitoring emerges as a critical tool in providing timely and accurate information about wildfires' location, size, and intensity, enabling efficient emergency response management and decision-making. However, existing remote sensing technologies, while valuable, face limitations such as coverage constraints and spatial-temporal resolution issues, hindering comprehensive

wildfire monitoring efforts. To address these challenges, recent advancements in artificial intelligence, particularly deep learning models, offer promising avenues for enhancing wildfire monitoring accuracy and efficiency.

Recent studies employing deep learning-based approaches have shown remarkable potential in early wildfire detection and monitoring, leveraging convolutional neural networks, recurrent neural networks, and time-series data analysis. Despite these advancements, current gaps in wildfire monitoring, such as the lack of fire boundary and intensity monitoring, highlight the need for further research and innovation to improve spatial resolution and operational capabilities. Through continued efforts and technological advancements, the development of prediction technologies holds the key to more effective wildfire management and mitigation strategies in the face of escalating wildfire risks [13].

6 EXISTING MACHINE LEARNING AND DEEP LEARNING APPLICATIONS IN WILDFIRE MONITORING

As wildfires continue to pose significant threats, the integration of machine learning to improve predictive abilities, allocate resources efficiently, and reduce wildfire impacts offers promising solutions across various tasks beyond forecasting. In this section, we'll delve into a range of machine learning tasks directed towards wildfire prediction, showcasing diverse methodologies and recent innovations.

6.1 WILDFIRE DETECTION AND EARLY WARNING SYSTEMS

Wildfire detection involves the early identification of wildfires to safeguard natural environments and is a significant challenge faced by government agencies and forest fire managers.

Detecting wildfires promptly reduces the need for human intervention and aids in monitoring and protecting remote areas that are difficult to access. One approach to this challenge involves the use of the Random Forest algorithm, a powerful machine learning technique known for its robustness in classification tasks. This method categorizes forest fires based on their size, texture, and rate of movement [18]. In addition to Random Forest, researchers have developed algorithms based on Convolutional Neural Networks (CNNs) to analyze satellite imagery and classify fire and non-fire regions accurately [19]. Furthermore, researchers have developed a cyber-physical system (CPS) integrating IoT sensors and autonomous unmanned aerial and ground vehicles controlled by the Robot Operating System. This system continuously monitors environmental conditions, enabling

early wildfire detection [20].

6.2 WILDFIRE OCCURRENCE PREDICTION

Wildfire occurrence prediction is the process of anticipating the number and location of fires starting in the near future, which is crucial for preparedness planning and resource allocation. As wildfires pose significant risks to both human lives and natural ecosystems, accurate prediction methods are essential for facilitating timely responses and minimizing potential damage. Traditionally, these predictions have relied on regression methods (traditional regression methods), but the introduction of machine learning (ML) techniques has revolutionized the field, offering more efficient and accurate prediction models.

Numerous studies have investigated the efficacy of machine learning (ML) methods in predicting wildfire occurrences. They tried using Artificial Neural Networks (ANNs) to forecast daily fire risk indices, incorporating diverse meteorological variables. They also tried Random Forest (RF) as a robust prediction tool. Researchers assessed various ML methods for predicting fire outbreaks, with RF showing good performance in predictive accuracy. Additionally, they explored integrating ML techniques with ensemble learning approaches to support prediction capabilities. They employed a two-stage ML approach, combining unsupervised deep learning methods with supervised ensemble classifiers to forecast bush-fire hot spot incidence. They found these methods effective [21].

6.3 FIRE SUSCEPTIBILITY MAPPING

Fire susceptibility mapping is a critical task that aims to predict the likelihood and distribution of fire occurrences within specific regions, aiding in fire risk assessment and mitigation strategies.

Machine learning (ML) algorithms, such as random forest (RF) and artificial neural networks (ANNs), have been widely employed for this task. RF models utilize landscape, climate, and anthropogenic variables to accurately map fire susceptibility, while ANNs offer enhanced predictive capabilities compared to traditional regression methods. Additionally, ensemble learning approaches combining multiple ML methods have shown promise in improving prediction accuracy. These methods provide valuable insights into temporal factors and regional variations in fire risk, enabling effective fire management strategies [21].

6.4 FIRE SPREAD AND GROWTH PREDICTION WITH MACHINE LEARNING

Predicting the spread of wildfires is crucial for effective fire management, aiding in resource allocation and evacuation planning. Machine learning (ML) techniques have been instrumental in enhancing the accuracy of fire spread predictions by leveraging historical data and environmental factors.

Researchers have explored various ML methods for fire spread prediction, including random forest (RF), artificial neural networks (ANNs), Bayesian networks (BNs), genetic algorithms (GAs), and convolutional neural networks (CNNs). RF classifiers have shown promise in identifying large fires accurately, while ANNs integrated with fuzzy logic models have been effective in estimating fire spread rates, particularly in challenging terrain. GAs have been utilized to optimize input parameters for physics-based fire spread simulators, resulting in improved prediction accuracy. Innovative approaches such as integrating Cellular Automata (CA) models with Extreme Learning Machines (ELM) have shown promise in simulating fire spread dynamics.

Recent advancements include the use of CNNs to predict fire spread using environmental variables, achieving high precision and sensitivity in predicting burn maps. These diverse ML approaches contribute to improved fire spread prediction capabilities, aiding fire management agencies in decision-making and proactive fire suppression efforts [21].

6.5 FINAL BURNED AREA PREDICTION

Initial studies compared multiple regression and various ML techniques, including Decision Trees (DT), Random Forest (RF), Artificial Neural Networks (ANN), and Support Vector Machines (SVM), to predict burned areas using fire and weather data [22]. Subsequent research built upon this foundation explored methods like genetic algorithms, hidden Markov models (HMM), and recurrent neural networks (RNN) to enhance prediction accuracy [21]. Furthermore, ML has been applied to classify fire sizes into different categories, transforming the burned area prediction problem into a classification task. Methods such as Self-Organizing Maps (SOMs) combined with ANNs and hybrid models integrating Fuzzy C-Means and Back-Propagation ANNs have demonstrated high accuracy in classifying fire size classes [23]. Studies comparing ML algorithms for estimating burned area and fire size classes have highlighted the effectiveness of techniques like extreme gradient boosting and deep learning, showcasing their potential in accurately predicting fire behavior [24].

Overall, these tasks represent significant advancements in wildfire monitoring and management. By leveraging the power of machine learning and deep learning techniques, such as convolutional neural networks, they enhance predictive accuracy, facilitate proactive resource allocation, and

more robust wildfire mitigation strategies.

7 CONCLUSION

In conclusion, wildfire is a complex issue with ecological, socioeconomic, and health implications. They can affect ecosystems, human health, and climate, and their uncontrolled spread poses risks to human populations, infrastructure, and the environment. Factors like meteorological conditions, human activities, and vegetation dynamics influence wildfire behavior. The recent surge in wildfires highlights the need for comprehensive understanding and interdisciplinary management. Advancements in machine learning and deep learning technologies can enhance wildfire monitoring accuracy, early detection, and prediction capabilities. A comprehensive and interdisciplinary approach is needed to manage wildfires effectively and minimize their impacts.

Turning to the next chapter, we will explore strategies used to tackle wildfire challenges, focusing on the role of machine learning in taking proactive measures.

CHAPTER 2

WILDFIRE FINAL BURNED AREA AND SIZE PREDICTION

1 INTRODUCTION

In the previous chapter, we explained how various factors interact, and we discussed numerous tasks involved in wildfire management, including wildfire occurrence prediction, wildfire susceptibility mapping, wildfire detection, early warning systems, and wildfire spread, to improve our understanding of wildfires. In this chapter, we will focus on two important tasks: predicting the final burned area and predicting the size of the wildfire. We will also discuss the significance of these tasks and review other research related to understanding wildfires, specifically focusing on burned areas and fire size. This chapter aims to provide a literature review of previous research and methodology.

2 PREDICTION OF FINAL BURNED AREA

A burned area is an area where wildfires have changed the structure of the vegetation, removed vegetation, and left ash and charcoal deposits. One of the most important tasks in predicting the effects of wildfires and taking preventive measures to reduce their effects is predicting burned areas. Predicting the final burned area refers to estimating the total extent of land that has been affected by a fire and determining the severity of the burn in different areas. Therefore, historical data, including wind direction, NDVI (Normalized Difference Vegetation Index), temperature, humidity, etc., is the information needed for this task to help in understanding the patterns and determining the spot of the burned area [25]. It is generally formulated as a semantic segmentation task, which involves assigning a class label to each pixel in an image to differentiate between burned and unburned areas. Deep learning (DL) models, such as the U-net architecture, U-net++ architecture, Deeplabv3 architecture, Deeplabv3+ architecture, Long Short-Term Memory (LSTM), or Recurrent Neural Network (RNN), are suggested for predicting burned areas.

2.1 WILDFIRE SIZE PREDICTION

In addition to estimating the burned areas, Estimating the extent of wildfires is essential for early response planning and resource allocation. The overall surface area impacted by the wildfire is represented by the burned area size, which is measured in hectares or square kilometers.

The area, measured in hectares, that Algerian wildfires destroyed between 2009 and 2023 is shown in The bar chart 2.1. With over 200,980 hectares burned, 2012 had the most recorded burned area, while 2018 had the lowest, at about 1,554 hectares.

Spatial models, Random Forests, and machine learning models such as BPNN, RNN, LSTM have been utilized. Including features such as temperature, wind, and humidity.

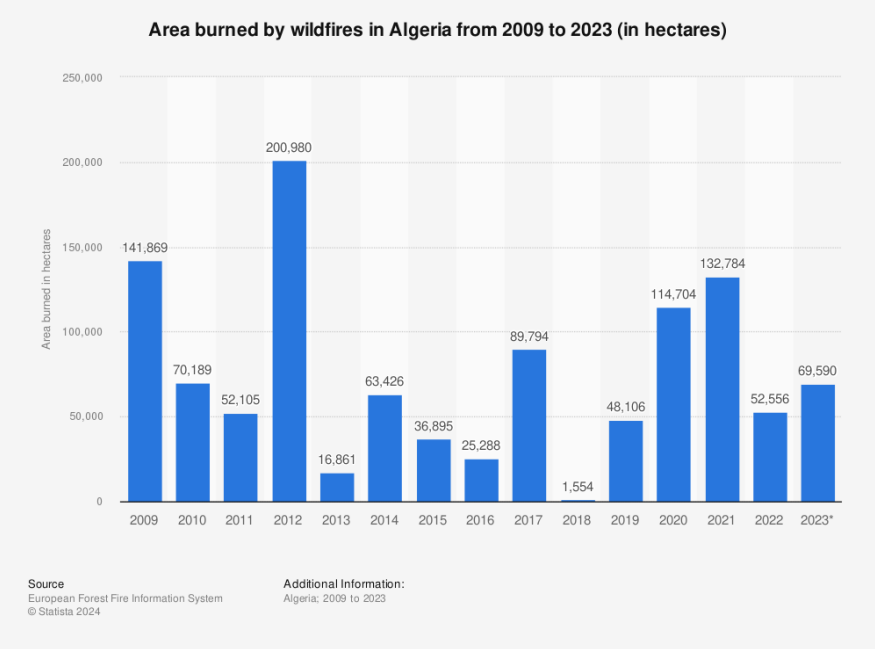

Figure 2.1: Area burned by wildfires in Algeria from 2009 to 2023 (in hectares)[1]

3 WHY IS IT SIGNIFICANT TO PREDICT WILDFIRE SIZE AND BURNT AREA?

By predicting the burned area and size of wildfires, we can protect the environment and wildlife from the impact of wildfires. This task helps us prepare for damages caused by categorizing areas based on their proneness to fires, specific plans can be developed for each area accordingly.
It allows us to develop specific plans for each area and estimate losses, such as the percentage of vegetation cover loss. We can also identify areas that are unsuitable for hiking or tourism due to the high frequency of fires.
Predicting fires in advance can also minimize economic damage. By understanding wildfire incidents, we can respond in an informed way and prevent their recurrence. Also helps assessing the damage to the ecosystem, and planning for recovery and restoration efforts.

[1]Source: https://www.statista.com/statistics/1281357/algeria-area-burned-by-wildfire/

4 RELATED WORKS

4.1 APPLICATION OF U-NET CONVOLUTIONAL NEURAL NETWORK TO BUSHFIRE MONITORING IN AUSTRALIA WITH SENTINEL-1/-2 DATA

The paper discusses the scale of devastation across four of the most populous states across Australia: New South Wales, Queensland, Victoria, and South Australia, which are more prone to wildfires. To predict burned areas with multispectral Sentinel-2 observations, clear skies are needed. Clouds or haze will hinder the process. It becomes difficult to locate affected regions of bushfire. used the U-Net deep learning framework for segmenting with Sentinel-1 SAR data [26]. However, there are limitations to the paper. There is a lack of knowledge about computational resources. We preferred to add metrics to the model's performance evaluation to compare it with other methods.

4.2 BURNED AREA MAPPING USING UNITEMPORAL PLANETSCOPE IMAGERY WITH A DEEP LEARNING-BASED APPROACH

The paper discusses a new burned area mapping method in Korea using PlanetScope imagery and U-Net architecture, This method used 17 satellite images for 12 forest fires, as well as labeled images. Band combination tests and topographic normalization improve classification accuracy. The results highlight the potential of deep learning-based approaches for detecting burned areas. The final image segmentation models exhibited F1 scores ranging from 0.883 to 0.939 and overall accuracies from 0.99 to 0.997 [27]. However, the paper has limitations. The model's ability for generalizability to different geographical regions is limited.

4.3 DOUBLE-STEP U-NET: A DEEP LEARNING-BASED APPROACH FOR THE ESTIMATION OF WILDFIRE DAMAGE SEVERITY THROUGH SENTINEL-2 SATELLITE DATA

This paper [28] discusses using deep learning to estimate the severity of wildfire damage. It uses data from Sentinel-2 satellites to create detailed images and also applies data augmentation techniques like rotation and flipping. The Double-Step U-net is a deep learning model that uses both classification and regression techniques. It assigns damage severity levels through classification and predicts values for each severity level through regression. The model provides a comprehensive assessment by dividing sub-areas into severity classes and offering detailed damage estimates within each class. To validate the model, data from 21 wildfires across five European countries was collected. The performance of the Double-Step U-Net, Parallel U-Net, and Simple U-Net in predicting

damage levels was compared with that of the dNBR-based solution. The paper has limitations, We must consider weather and other factors because they play an important role and cannot be ignored. These factors are critical and must be considered.

4.4 PREDICTING WILDFIRE BURNED AREA IN SOUTH CENTRAL US USING INTEGRATED MACHINE LEARNING TECHNIQUES

This study [29] discusses predicting wildfire burned areas in the United States, specifically the South Central United States during 2002–2015, by the use of integrated machine learning methods. Used three specific geospatial variables on a monthly basis. These variables included land coverage categories, ecoregions categories, and 2010 population density data. he used machine learning algorithms, such as Random Forests , Gradient Boosting Machines , Support Vector Machines , and Neural Networks . as results The AUC values of 0.82 and 0.83 were achieved by the models for different seasons. The paper's focus on the U S States could limit the model's effectiveness for other areas with changing ecological and climatic conditions.

4.5 UNI-TEMPORAL MULTISPECTRAL IMAGERY FOR BURNED AREA MAPPING WITH DEEP LEARNING

This study [30] explores the use of deep learning techniques for mapping burned areas using uni-temporal multispectral imagery. data used Sentinel-2 imagery and Landsat-8 imagery for mapping burned areas using deep learning (DL) models including U-Net, HRNet, Fast-SCNN, and DeepLabv3+ and machine learning (ML) algorithms including KNN, Random Forest, and LightGBM, When comparing deep learning (DL) models and machine learning (ML) algorithms for mapping burned areas from uni-temporal multispectral imagery in various wildfire sites, it was found that DL algorithms outperformed ML methods, particularly in cases with compact burned scars. HRNet performed well when transferring the trained models to Landsat-8 data.

4.6 ESTIMATION OF THE BURNED AREA IN FOREST FIRES USING COMPUTATIONAL INTELLIGENCE TECHNIQUES

This study [31] has estimated the size of forest fires through the use of data from Turkey's Department of Forestry, comprising 7,920 fires between 2000 and 2009. This encompasses a number of features, which include tree species, meteorological details, fire dates and geographical conditions.

Such estimation approaches like fuzzy logic, multilayer perceptrons, radial basis function networks, and support vector machines were utilized.

4.7 ASSESSMENT OF BURNED AREAS DURING THE PANTANAL FIRE CRISIS IN 2020 USING SENTINEL-2 IMAGES

This research [32] employed Sentinel-2 MSI images to map the extent of burned areas. This took place during a specific fire incident within Brazilian Pantanal biome in 2020. Google Earth Engine was used as a platform and random forest machine learning algorithm was applied with input variables obtained from SENTINEL 2 data including shade fraction, NBR, and NDVI images. The overall accuracy is 95.9 and predicted an extensive burnt region of about 44,998 km^2 indicative of significant loss of biodiversity and massive ecosystem destruction that occurred. It should be noted that this estimate surpassed other existing burnt area products due to disparate datasets and methodologies employed. However, this study has some limitations which must be highlighted One potential limitation may relate to satellite imagery which may have difficulties capturing all burned areas especially in cases where there is dense vegetation or cloud coverage obstructing the image.

4.8 DEEP LEARNING BASED BURNT AREA MAPPING USING SENTINEL 1 FOR THE SANTA CRUZ MOUNTAINS LIGHTNING COMPLEX (CZU) AND CREEK FIRES 2020

The research builds upon existing SAR (Synthetic Aperture Radar) burnt area estimation models by introducing a novel approach that combines a U-Net with ResNet50 architecture for more accurate burnt area mapping. This contribution extends the capabilities of SAR data applications in Earth observation, providing valuable insights for resource managers to respond effectively to natural disasters.

The study utilizes SAR (Synthetic Aperture Radar), Digital Elevation Model (DEM), and land cover data to map burned areas. Methodologically, the study employs a U-Net combined with ResNet50 architecture. The study achieves significant results, attaining a maximum burnt area segmentation F1-Score of 0.671, surpassing existing models. It introduces three models for burnt area mapping: U-Net with a ResNet50 Encoder Architecture, Encoder-Decoder Network with Pseudo Labels, and Additional Channels Model. These models are evaluated using quantitative metrics like Accuracy, Precision, Recall, and F1-Score, with the primary model demonstrating superior performance.

However, the study acknowledges limitations, particularly those related to input data accuracy, data labeling precision, challenges associated with data augmentation techniques where a Gaussian blur

was utilized in the study to enhance the generalization capability of the model which, if not carefully controlled, could introduce further noise and potentially hinder the model's effectiveness [33].

4.9 MACHINE LEARNING TO PREDICT FINAL FIRE SIZE AT THE TIME OF IGNITION

The study conducted a predictive analysis of final fire size at the time of ignition in Boreal forests in Alaska, aiming to assist fire management efforts in mitigating the escalating fire activity attributed to climate change.

The research utilized meteorological data from the European Centre for Medium-Range Weather Forecasts (ECMWF) ERA5 reanalysis, including 2-meter air temperature, relative humidity, precipitation, 10-meter wind speed, and surface air pressure at a 0.25° resolution. Decision trees were the main model used in the study. These decision trees were tasked with classifying ignitions into small, medium, or large fires, achieving an accuracy rate of 50.4%. Key variables used in the classification process included the vapor pressure deficit and the fraction of spruce cover near the ignition point. Notably, the model forecasted that 40% of ignitions would result in large fires, responsible for 75% of the total burned area. While other machine learning algorithms were trialed, none surpassed the decision tree model's performance.

The model demonstrated early identification capabilities for large fires, boasting a recall rate of 65% and a precision rate of 53% [34]. However, certain limitations were acknowledged, including the potential for overprediction of large fires in areas with intensive human management practices. Moreover, the model's efficacy might vary across different ecosystems or under extreme weather conditions not accounted for in the available data.

4.10 A DEEP LEARNING APPROACH FOR BURNED AREA SEGMENTATION WITH SENTINEL-2 DATA

The paper addresses the critical need for accurate burned area segmentation, recognizing the significant ecological, social, and economic impacts of wildfires.

The study utilizes mono-temporal Sentinel-2 imagery for burned area segmentation and introduces a new training and validation dataset tailored for training a convolutional neural network based on a U-Net architecture. This architecture leverages spectral bands from the visual, near-infrared, and shortwave infrared domains to achieve optimal network performance.

The final segmentation model demonstrates an overall accuracy of 0.98 and a kappa coefficient of 0.94, highlighting the efficacy of the proposed deep learning approach for burned area segmentation [35].

However, the research paper does not explicitly mention the specific loss function used for training the convolutional neural network, which warrants further investigation for a comprehensive understanding of the model's training process and performance. Additionally, the study focuses solely on analyzing and segmenting burned areas based on the spectral information present in Sentinel-2 imagery, without considering external factors such as meteorological conditions or vegetation characteristics.

4.11 SEMANTIC SEGMENTATION OF BURNED AREAS IN SATELLITE IMAGES USING A U-NET-BASED CONVOLUTIONAL NEURAL NETWORK

The study conducted by Brand and Manandhar investigates the utilization of deep learning techniques, specifically a U-Net variant, to address the shortcomings of traditional methods in remote sensing for mapping burned areas in satellite imagery.

Through semantic segmentation, the paper highlights the evolution in remote sensing techniques and the shift towards deep learning for more accurate burned area mapping. Leveraging mono-temporal Sentinel-2 imagery, the study trains two variants of the U-Net model: a local model, trained on specific research area data, and a global model, trained on the entire dataset. Performance evaluation metrics such as overall accuracy and macro-F1 score are employed to assess the models' effectiveness. The study optimized the neural network using Binary Cross-Entropy (BCE) as the loss function. The selection of the U-Net architecture stems from its proven efficacy in semantic segmentation tasks, particularly in handling spatial data inherent in satellite imagery. Customized to suit the study's objectives, the U-Net model demonstrates robust generalization across diverse research areas, with the global model exhibiting superior performance. Despite its successes, the model faces limitations, such as misclassifications in certain land cover classes, including bare soil, which highlight the need for further refinement and optimization [36]. Additionally, the study does not explicitly consider external factors such as meteorological conditions or vegetation characteristics in the analysis and modeling process.

4.12 MESOGEOS: A MULTI-PURPOSE DATASET FOR DATA-DRIVEN WILDFIRE MODELING IN THE MEDITERRANEAN, FINAL BURNED AREA PREDICTION

The study conducted by the researchers aims to accurately predict the extent of burned areas following a wildfire event. Previous research has underscored the significant impact of meteorology, vegetation characteristics, and human activities on the spread and size of burned areas, necessitating more robust modeling approaches. In this context, the study leverages machine learning (ML)

techniques to enhance the accuracy of the final burned area prediction. To achieve this objective, the researchers utilize the Mesogeos dataset, which integrates crucial variables such as meteorology, vegetation, human activity, historical wildfire records, and other relevant factors. A standard U-Net model was used with an EfficientNet-B1 Encoder trained on comprehensive historical records of wildfire ignitions and burned areas spanning from 2006 to 2022. The optimization process employs Binary Cross-Entropy (BCE) as the objective function [3]. However, the choice of Binary Cross-Entropy (BCE) as the loss function struggles with the imbalanced nature of the wildfire data, where burned areas are much less common than unburned areas. This imbalance can lead to a model biased towards predicting unburned areas, reducing its accuracy in detecting burned regions. Furthermore, the researchers did not sufficiently address the issue of class imbalance in their data, which is critical for improving prediction accuracy in wildfire modeling. Improving the model's accuracy in predicting burned areas, despite the predominance of unburned regions, is crucial for better wildfire management.

5 CONCLUSION

In conclusion, this chapter delved into the prediction of burned areas and wildfire sizes, emphasizing their importance. We explained previous studies that employed a variety of deep learning models, such as U-Net, U-Net++, Deeplabv3, and LSTM or RNN. Nevertheless, these studies encountered limitations, like the difficulty of generalizing the models to diverse geographical areas.

In the next chapter, we will describe the dataset structure and the types of data it contains. Additionally, we will explain the methods used to process and analyze this data, including a comparative study of three different models using various deep learning methods.

CHAPTER 3

CONTRIBUTION 1: COMPARATIVE ANALYSIS OF SOME U-NET VARIANTS FOR BURNED AREA PREDICTION

1 INTRODUCTION

In the previous chapter, we discussed tasks for predicting burned areas and wildfire size, as well as the related work for these tasks and why they are important.

In this chapter, we will explain the dataset and methodology used for wildfire prediction. The Mesogeos dataset is a helpful source for using data to predict wildfires in the Mediterranean, specifically focusing on predicting the burned area and the size of the fire. We will describe the structure of the dataset and the types of data it contains. This will include detailed information on variables such as burned areas, curvature, ignition points, wind direction, and wind speed.

Furthermore, we will explain the methods used to estimate the likelihood of neighboring pixels around the ignition point being included within the final burned area. This includes an in-depth look at U-net, U-Net++, and Dense-Unet comparing their effectiveness in predicting burned areas. By examining metrics like F1-score and AUPRC, we aim to determine which model performs best. The objective of this research is to develop robust models that can predict wildfire behavior with high precision, thereby aiding in effective wildfire management and mitigation efforts.

2 DATA COLLECTION

In our research centered around wildfire modeling, we face the challenge of accessing suitable datasets essential for effectively leveraging Deep Learning (DL) techniques.

Finding large datasets to support projects like wildfire modeling is indeed a significant challenge. Data on wildfires is dispersed across various sources, in different formats, and at different levels of detail. Hours are spent searching countless sources, only to encounter inaccessible or poorly generalized datasets.

However, we turn to Mesogeos [3], a newly published dataset in the NeurIPS 2023 Datasets and Benchmarks Track[1]. Mesogeos is an extensive and versatile dataset meticulously designed to support various Machine Learning (ML) applications in wildfire modeling within the Mediterranean region.

2.1 MESOGEOS

Mesogeos, a multi-purpose data tailored for data-driven wildfire modeling in the Mediterranean region [3]. Mesogeos integrates crucial variables such as meteorological conditions, vegetation

[1]Source: https://nips.cc/

characteristics, and human activities, along with historical wildfire occurrence data spanning a 17-year period from 2006 to 2022. Structured as a cloud-friendly spatio-temporal datacube with a resolution of 1km x 1km x 1-day (daily resolution), spanning an area of 4714km x 1753km over 6026 days.

The Mesogeos dataset is created by collecting data from diverse sources. These inputs undergo extensive pre-processing, including interpolation, aggregation, calculation of new variables, and rasterization. Subsequently, the processed data is organized into daily chunks and appended to the datacube based on the corresponding date.This comprehensive approach ensures that the Mesogeos dataset captures the complexity of wildfire dynamics in the Mediterranean region.

This structured dataset supports machine learning applications, aiding in wildfire risk prediction and mitigation efforts.

The Mesogeos Datacube, organized in a three-dimensional format consisting of longitude, latitude, and time, comprises 27 variables representing factors influencing wildfires.

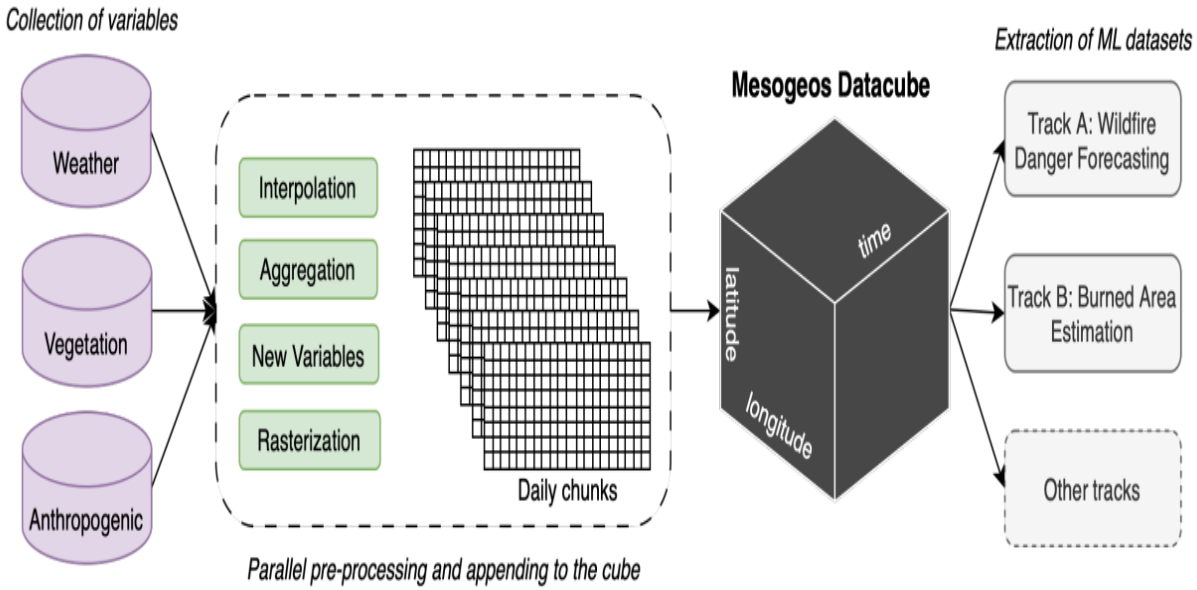

Figure 3.1: Pipeline of the datacube construction [3].

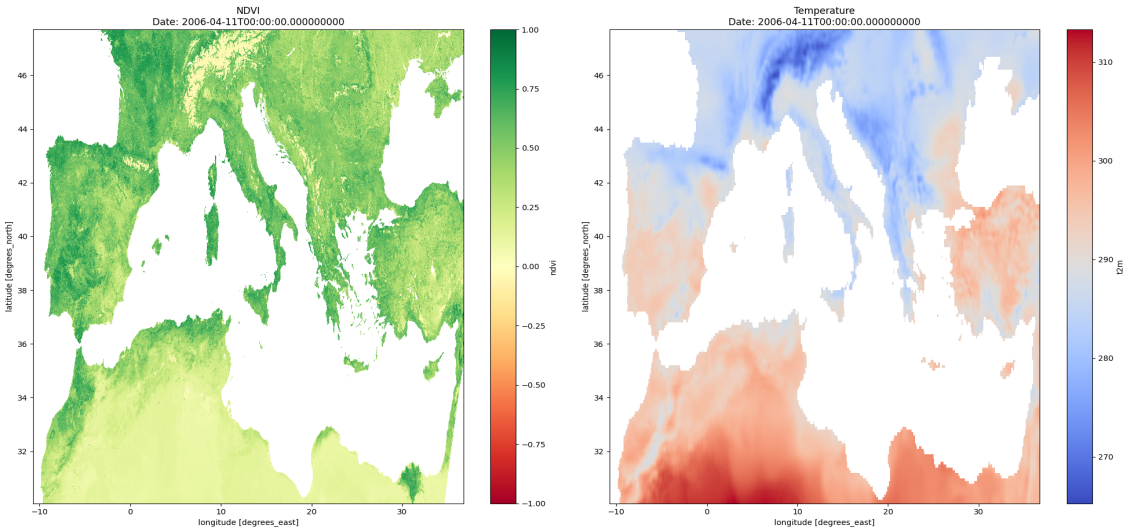

Figure 3.2: Visualization of some variables for a day. (Left: NDVI variable, Right: Temperature variable)

2.2 FINAL BURNED AREA PREDICTION DATASET

Mesogeos facilitates machine learning techniques for various wildfire modeling tasks. Notably, two machine learning-ready datasets derived from Mesogeos focus on short-term wildfire risk prediction and estimating the extent of burned areas from ignition points.

Since our primary interest lies in predicting the final burned area, we will turn our attention to the second dataset specifically designed for this purpose. This dataset involves extracting 64km $\times$ 64km patches centered around each fire's ignition point, typically capturing the entire burned area. Each sample includes the values of all relevant variables from the datacube on the date the fire occurred, providing detailed context for each fire event.

The dataset includes individual samples organized by year, denoted as

$$"YYYY/sample\_XXX.nc"$$

where "$YYYY$" represents the year and "XXX" is the sample number. Each sample, stored in NetCDF format[2], represents a snapshot of environmental conditions surrounding wildfire events for a specific year.

Below, a table providing information about the available variables in the NetCDF file, including their dimensions and shape.

[2]For more information on NetCDF, visit NetCDF

No.	Variable Name	Variable Explanation	Dimensions	Shape
1	Aspect	Slope direction indicator	('y', 'x')	(64, 64)
2	Burned Areas	Fire affected regions	('time', 'y', 'x')	(1, 64, 64)
3	Curvature	Terrain shape measure	('y', 'x')	(64, 64)
4	D2M	Dew point temperature	('time', 'y', 'x')	(1, 64, 64)
5	DEM	Elevation model data	('y', 'x')	(64, 64)
6	Ignition Points	Fire start locations	('time', 'y', 'x')	(1, 64, 64)
7	LAI (Leaf Area Index)	Vegetation density measure	('time', 'y', 'x')	(1, 64, 64)
8	LST Day	Daytime land temperature	('time', 'y', 'x')	(1, 64, 64)
9	LST Night	Nighttime land temperature	('time', 'y', 'x')	(1, 64, 64)
10	NDVI	Vegetation health index	('time', 'y', 'x')	(1, 64, 64)
11	RH (Relative Humidity)	Air moisture level	('time', 'y', 'x')	(1, 64, 64)
12	Roads Distance	Proximity to roads	('y', 'x')	(64, 64)
13	Slope	Terrain steepness measure	('y', 'x')	(64, 64)
14	SMI (Soil Moisture Index)	Soil wetness measure	('time', 'y', 'x')	(1, 64, 64)
15	SP (Surface Pressure)	Atmospheric pressure data	('time', 'y', 'x')	(1, 64, 64)
16	Spatial Reference	Geolocation information	/	/
17	SSRD	Solar radiation data	('time', 'y', 'x')	(1, 64, 64)
18	T2M	Air temperature data	('time', 'y', 'x')	(1, 64, 64)
19	Time	Temporal information	/	/
20	TP (Total Precipitation)	Rainfall measure	('time', 'y', 'x')	(1, 64, 64)
21	Wind Direction	Wind direction data	('time', 'y', 'x')	(1, 64, 64)
22	Wind Speed	Wind velocity data	('time', 'y', 'x')	(1, 64, 64)
23	Land Cover - Agriculture	Agricultural land areas	('y', 'x')	(64, 64)
24	Land Cover - Forest	Forested areas	('y', 'x')	(64, 64)

No.	Variable Name	Variable Explanation	Dimensions	Shape
25	Land Cover - Grassland	Grass-covered areas	('y', 'x')	(64, 64)
26	Land Cover - Settlement	Urban areas	('y', 'x')	(64, 64)
27	Land Cover - Shrubland	Shrubby areas	('y', 'x')	(64, 64)
28	Land Cover - Sparse Vegetation	Sparse vegetation areas	('y', 'x')	(64, 64)
29	Land Cover - Water Bodies	Water-covered areas	('y', 'x')	(64, 64)
30	Land Cover - Wetland	Wetland areas	('y', 'x')	(64, 64)
31	Population	Human population density	('y', 'x')	(64, 64)

Table 3.1: Data Variables Information

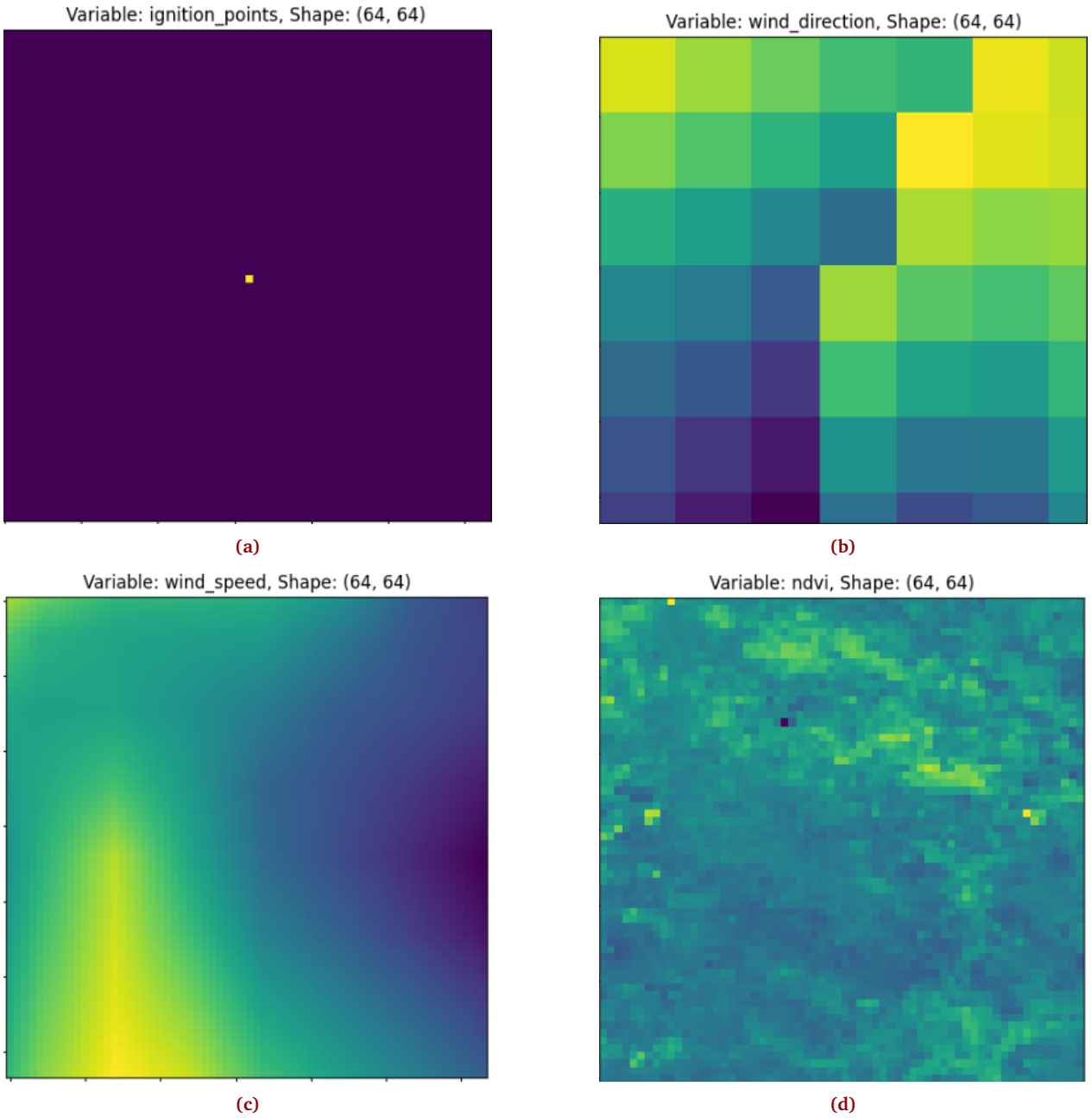

Figure 3.3: some variables samples, (a) : ignition point , (b) : roads distance , (c): wind speed , (d): NDVI

2.3 PREPROCESSING OF THE DATASET

To ensure the dataset is in a suitable format for analysis and modeling, a comprehensive preprocessing was implemented. The steps involved in this preprocessing are outlined below.

Initially, the dataset, which is stored in NetCDF files, was organized by year. The preprocessing began by loading data from each year's folder. For each file within these folders, the dataset was opened, and relevant variables were extracted. These variables included a combination of features and target variable. The features were gathered into a collective dataset, while the "burned_areas" variable served as the target variable, during this process, the dimensionality of the time was removed. Before proceeding with further data processing, any missing values (NaNs) in the dataset were replaced with the nearest value to the missing one. This step ensured that the dataset was complete and that subsequent operations would not encounter issues due to missing data.

To normalize the feature data, a Min-Max scaling technique was applied. This process ensures that all feature values are scaled to a range between 0 and 1, which is crucial to function optimally. This normalization process helps in reducing bias due to differing scales of the variables. The MinMaxScaler[3] from the scikit-learn library was employed.

The preprocessed data was then divided into training, validation, and testing sets. Initially, we organized our data into a train-test split based on temporal ordering, with earlier years designated for training and the most recent year reserved for testing. However, to enhance the robustness of our models and ensure exposure to diverse scenarios, we later transitioned to utilizing random train validation and test subsets. This approach allows models to learn from varied data distributions and generalize more effectively to unseen instances. This was achieved using a (70,10,20) split, where 70% of the data was allocated for training, 10% for validation, and 20% for testing. This split helps in validating the model's performance on unseen data, ensuring that it generalizes well.

Given the dataset's complexity and size, we selected a subset of years. This selection process was crucial due to **memory limitations** encountered during our initial attempts, which often resulted in frequent runtime disconnections and memory crashes.

This systematic approach ensured that the data was clean, normalized, and ready for subsequent modeling and analysis tasks. The preprocessing steps were crucial in enhancing the quality of the data and ensuring that the machine learning models built on this data would perform reliably and accurately.

[3]For more information on the MinMaxScaler and its usage, please refer to the official documentation provided by scikit-learn.

2.4 DATASET IMBALANCE ANALYSIS

During the preprocessing and initial analysis of the dataset, it became evident that there is a significant imbalance between the burned areas regions and the non-burned areas regions. To quantify this imbalance, the ratios of burned areas regions and non-burned areas regions were calculated.

The formula used to calculate these ratios is as follows:

$$\text{Burned Area Ratio} = \frac{\text{Number of Burned Area Pixels}}{\text{Total Number of Pixels}} \tag{3.1}$$

$$\text{Non-Burned Area Ratio} = \frac{\text{Number of Non-Burned Area Pixels}}{\text{Total Number of Pixels}} \tag{3.2}$$

Where:

- **Total Number of Pixels**: Total Number of Pixels is the sum of all pixels in sample.
- **Number of Burned Area Pixels**: Number of Burned Area Pixels is the count of pixels identified as burned areas.
- **Number of Non-Burned Area Pixels**: Number of Non-Burned Area Pixels is the count of pixels identified as non-burned areas, which can be calculated as the difference between the total number of pixels and the number of burned area pixels.

Using these formulas, the ratios were computed, and the results are as follows:

$$\text{Mean Burned Area Ratio} \approx 0.0055$$

$$\text{Mean Non-Burned Area Ratio} \approx 0.9945$$

This means that burned area pixels constitute approximately 0.55% of the dataset, whereas non-burned area pixels make up about 99.45%. This significant imbalance indicates that the dataset is heavily skewed towards non-burned areas, making the dataset **extremely challenging**. Addressing this imbalance is crucial for building a robust machine learning model, as many algorithms may perform poorly when trained on imbalanced data.

3 U-NET ARCHITECTURE

A convolutional neural network (CNN) is a class of artificial neural network commonly used for analyzing images. It is a multi-layer architecture that uses layers of filters to extract features and details from images, enabling tasks such as classification, recognition, and segmentation [37]. The U-Net architecture 3.4 is a convolutional neural network (CNN) designed for a variety of tasks, including image segmentation. This architecture consists of two main parts: an encoder and a decoder [38]. We can apply the U-Net in a wide range of domains, especially in the medical field. Where its application includes brain tumor segmentation [39] and skin lesion segmentation [40], satellite imagery segmentation [41]. U-Net variants include Attention U-net, 3D U-net, dense U-net, U-net++, residual U-net, and Adversarial U-net [42].

3.1 ENCODER

The encoder (contracting path) is designed to capture context and extract features. It consists of repeated blocks where two 3x3 unpadded convolutions are used, each followed by a rectified linear unit (ReLU) activation function. These convolutional operations are then followed by a 2x2 max pooling operation with a stride of 2, which reduces the size of the feature maps while increasing the number of feature channels. This process continues through several layers, effectively capturing high-level features while reducing the spatial resolution [4].

3.2 DECODER

The decoder (expansive path) reconstructs the image using high-level features from the encoder (contracting path). It uses a sequence of upsampling steps to increase the spatial resolution. In each step, the feature map is upsampled and then reduced by half using a 2x2 convolution. The upsampled feature map is combined with the corresponding feature map from the contracting path and then two 3x3 convolutions, each followed by a ReLU activation. This process allows the network to combine high-level abstract features with localized information from earlier layers, enabling precise localization and segmentation [4].

Finally, in the last layer, a 1x1 convolution is used to map the processed features to the desired number of output classes [4].

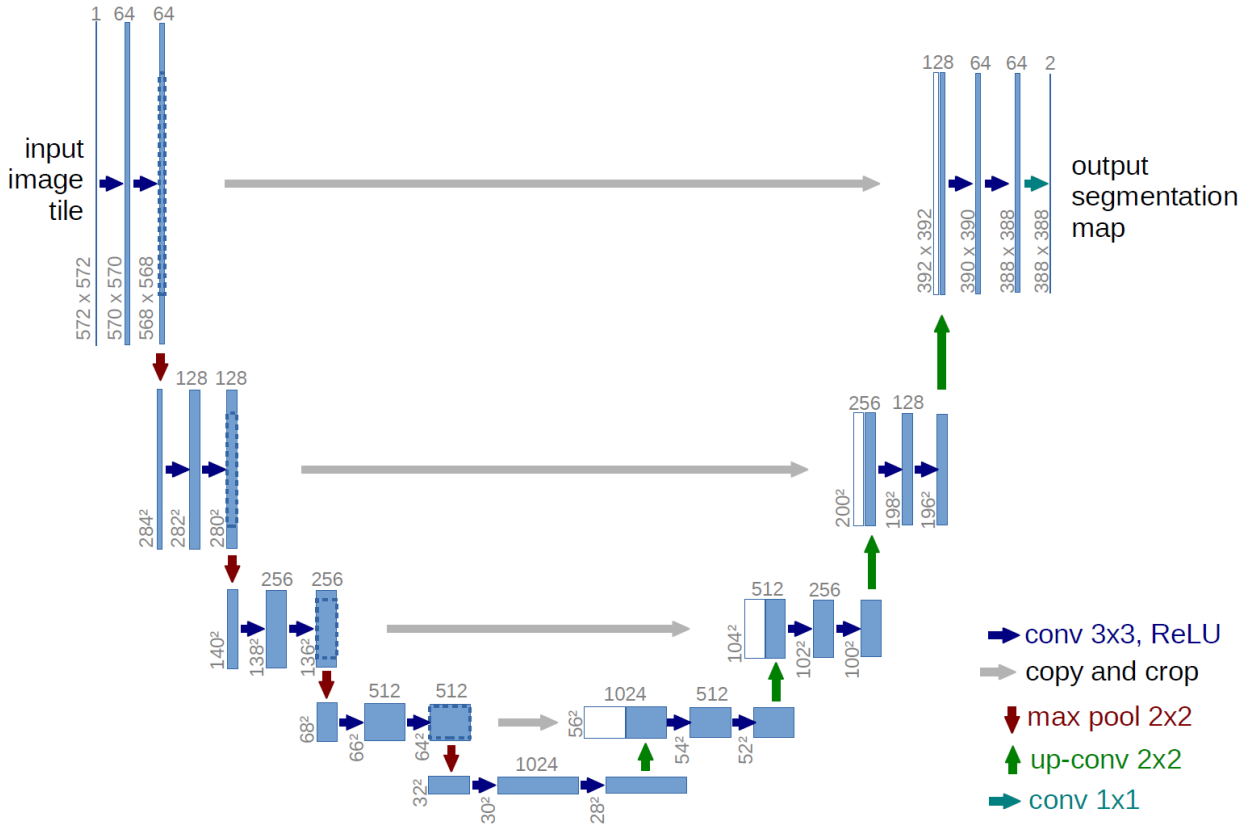

Figure 3.4: U-net architecture [4]

4 U-NET++ ARCHITECTURE

U-Net++ architecture [5] is an advanced deep learning architecture for image segmentation that builds upon the original U-Net model [4]. It introduces innovative feature to address some of the limitations of U-Net, particularly the semantic gap between encoder and decoder feature maps.
UNet++ introduces **nested dense skip connections**. The nested dense skip connections between the encoder and decoder at multiple levels enhance the flow of information and bridge the semantic gap, resulting in more accurate segmentation.

4.1 RE-DESIGNED SKIP PATHWAYS

The primary innovation in UNet++ is the re-designed skip pathways that connect the encoder and decoder through dense convolution blocks. Unlike U-Net [4], where the encoder's feature maps are directly transferred to the decoder, UNet++ introduces dense convolution blocks within these skip pathways.
Each dense convolution block contains multiple convolution layers, with the number of layers depending on the pyramid level, or the depth within the network hierarchy. Each layer in this block concatenates the output from the previous layer with the up-sampled output from a lower dense block. This process ensures that the encoder feature maps are semantically richer and more closely aligned with the decoder feature maps, thus simplifying the optimization problem for the network.

An instance of bridging the semantic gap is demonstrated in figure 3.5 between $(\mathbf{X_{0,0}}, \mathbf{X_{2,2}})$ by employing a dense convolution block comprising three convolution layers.
This alignment is hypothesized to facilitate optimization, as similar semantic features ease the learning process for the optimizer. The skip pathway is formally defined, where the output of each node is computed based on the convolution and up-sampling operations. The dense convolution block ensures that all prior feature maps accumulate and contribute to the current node's output. The nested dense skip connections allow the model to aggregate multi-level features, resulting in more precise and accurate segmentation maps. Figure from the original paper visually illustrates the process of feature maps traversing the first skip pathway of UNet++.

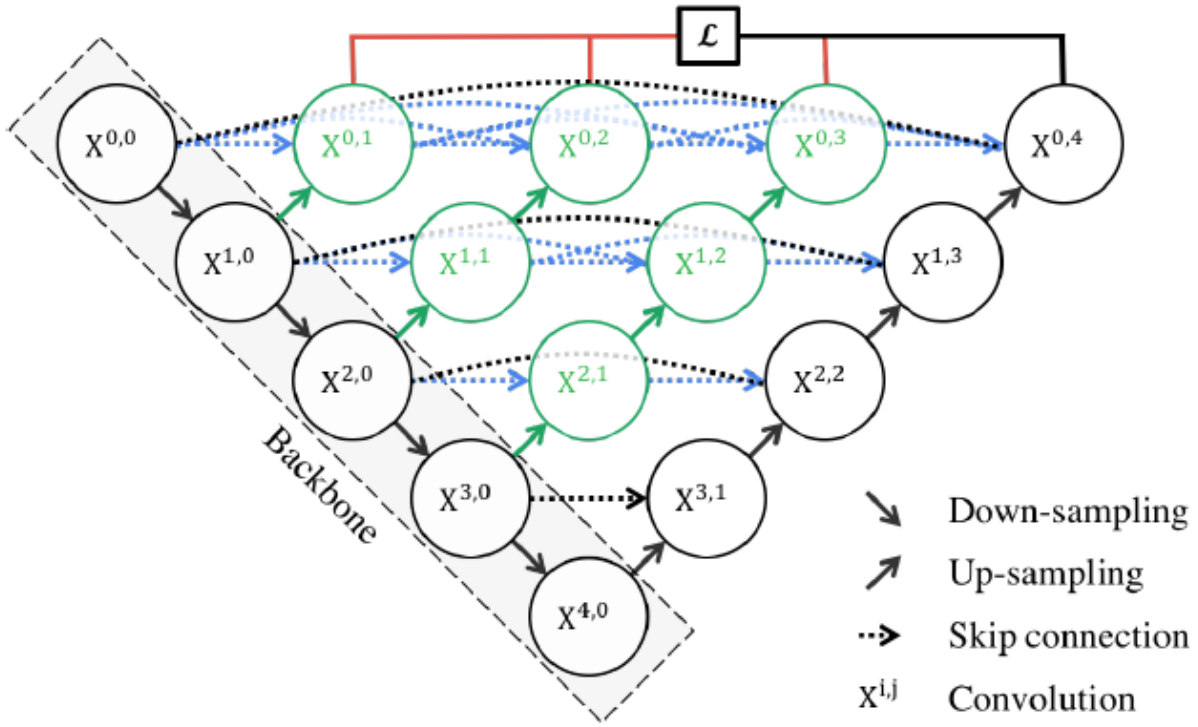

Figure 3.5: Graphical Abstract of UNet++: Original U-Net Components in Black, Dense Convolution Blocks in Green and Blue, and Deep Supervision in Red [5]

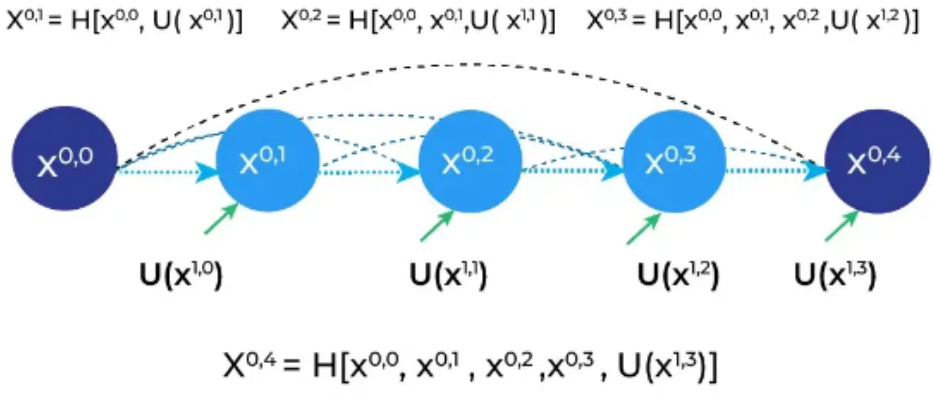

Figure 3.6: Nested Skip Pathways[4]

[4]Source: https://www.geeksforgeeks.org/unet-architecture-explained/

5 DENSE U-NET ARCHITECTURE

The dense U-net architecture 3.7 is constructed by integrating the U-net with dense concatenation. The Dense-UNet architecture has a dense downsampling path and a dense upsampling path. These paths are symmetrical, and they have skip connection channels to link them together [6]

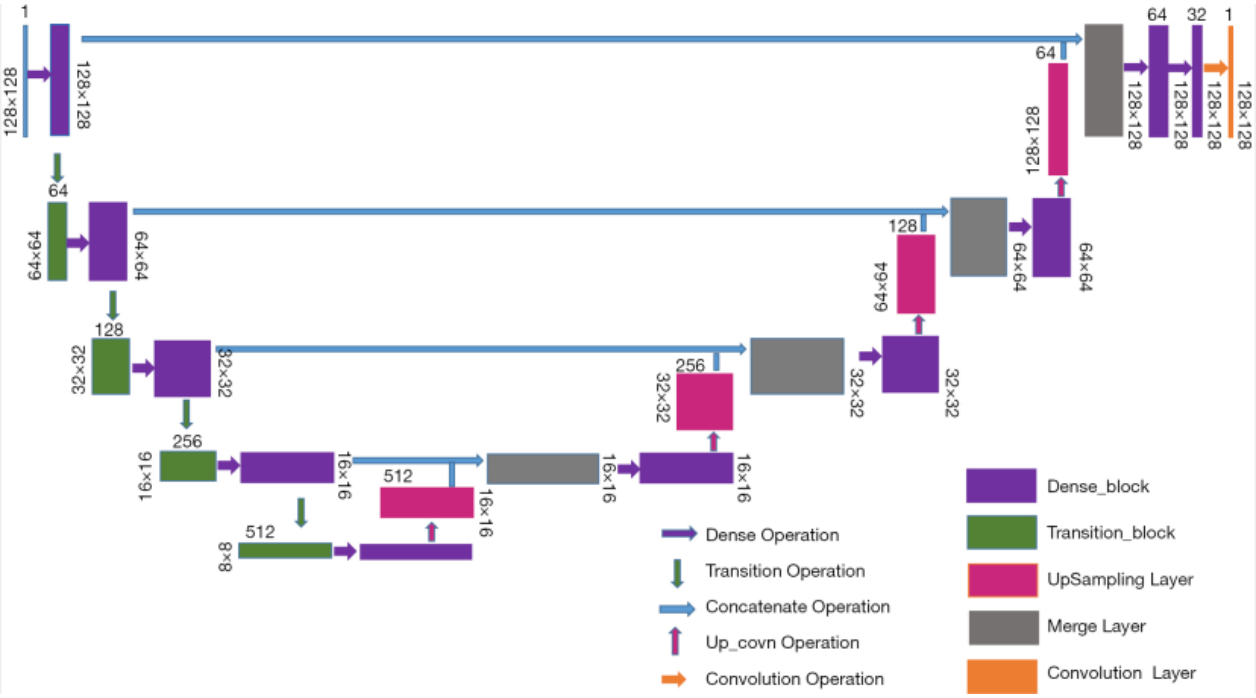

Figure 3.7: Dense U-net architecture [6]

5.1 DOWNSAMPLING PATH

Downsampling path is designed to capture semantic contextual features on multiple scales. with input at a resolution of (128×128×3), and goes through four downsampling layers to extract local features. In order to make the traditional U-Net architecture deeper, standard pooling and convolution operations are replaced with dense-block as shown in 3.8 and transition-block 3.9 operations. Each dense-block contains four densely connected layers, creating a feed-forward link to all preceding layers, known as dense concatenation. This design maximizes feature reuse and ensures that the feature maps in each layer maintain the same size. The dense downsampling path consists of five layers, each containing a dense-block and a transition-block 3.9, resulting in a total of five dense-blocks in this path. These adjustments significantly increase the network's depth, improving its ability to capture complex features from the input images [6].

5.2 UPSAMPLING PATH

upsampling path reconstructs images with high-resolution from the compressed features obtained in the downsampling path. This path reverses the structure of the downsampling path, with the goal of recovering the full input resolution while accurately localizing specific regions. It consists of five layers, each using dense blocks, upsampling layers, and merger operations. Like the dense downsampling path, each dense block in the upsampling path contains four densely connected layers to ensure extensive feature reuse. The upsampling layers gradually increase the spatial dimensions of the feature maps, while merger operations help combine features from different layers for precise localization. Although the dense block replaces the standard convolution operations, the overall upsampling mechanism retains the core principles of the U-Net architecture. This path, comprising five dense blocks, effectively reconstructs high-resolution images, ensuring that the network delivers detailed and accurate outputs [6].

The use of a Dense block (DB) 3.8 in a dense U-net to address the vanishing gradient problem. The DB is applied to the network to solve the vanishing gradient problem by connecting each feature map with dense connectivity. The DB encourages the reuse of features and ensures that all layers in the architecture receive a direct supervision signal. By applying the DB, the network can improve information flow and solve the vanishing-gradient problem, leading to high segmentation accuracy [43].

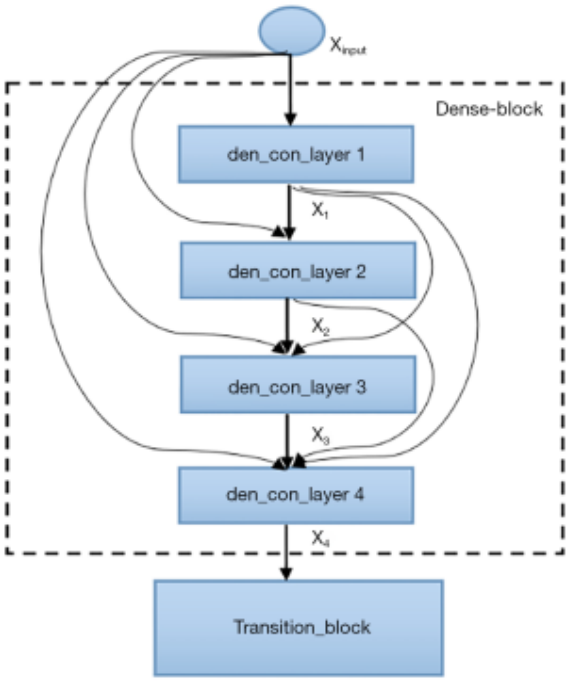

Figure 3.8: Dense Block [6]

Figure 3.9: Transition Block [6]

Figure 3.10: Den-Con Layer [6]

6 EVALUATION METRICS

6.1 F1-SCORE

The F-measure, often referred to as the F1-score, serves as a fundamental metric in classification tasks, providing a balanced evaluation of precision and recall Precision, denoted as Precision $= \frac{TP}{TP+FP}$, represents the ratio of true positives to the sum of true positives and false positives, while recall, defined as Recall $= \frac{TP}{TP+FN}$, signifies the ratio of true positives to the sum of true positives and false negatives. By computing the harmonic mean of these two metrics, the F-measure offers insights into a model's performance across different thresholds. With values ranging from zero to one, higher F1-scores signify more effective classification capabilities [44]. The F-1 score is very useful when dealing with imbalanced class problems. The F1 score provides a balanced assessment by taking into account both false positives and false negatives, making it robust in scenarios where class distribution is skewed as it offers a comprehensive evaluation that is not biased towards the

majority class. It is expressed as:

$$F_{\text{measure}} = \frac{2 \times \text{PPV} \times \text{TPR}}{\text{PPV} + \text{TPR}} = \frac{2 \times \text{TP}}{2 \times \text{TP} + \text{FP} + \text{FN}}$$

6.2 DICE COEFFICIENT

The Dice coefficient (DC) is a measure used to quantify the similarity between two binary regions. It is traditionally employed to compare a ground truth binary image with a probabilistic map [45]. The Dice coefficient (DC) is typically calculated using the formula:

$$DC = \frac{2 * |A \cap B|}{|A| + |B|}$$

A is a set representing the ground truth, while B represents the computed segmentation. Both images (sets) are binary, with values '0' or '1' assigned to each pixel.

6.3 THE PRECISION-RECALL CURVE

The Precision-Recall (PR) curve is a graphical tool used to evaluate the performance of binary classifiers, especially in the context of imbalanced datasets. It plots precision (the proportion of true positive predictions among all positive predictions) against recall (the proportion of true positive predictions among all actual positive instances) [46].

Below is the figure that shows examples of PR curves for the output of a binary classifier at various levels of separation and positive rates.

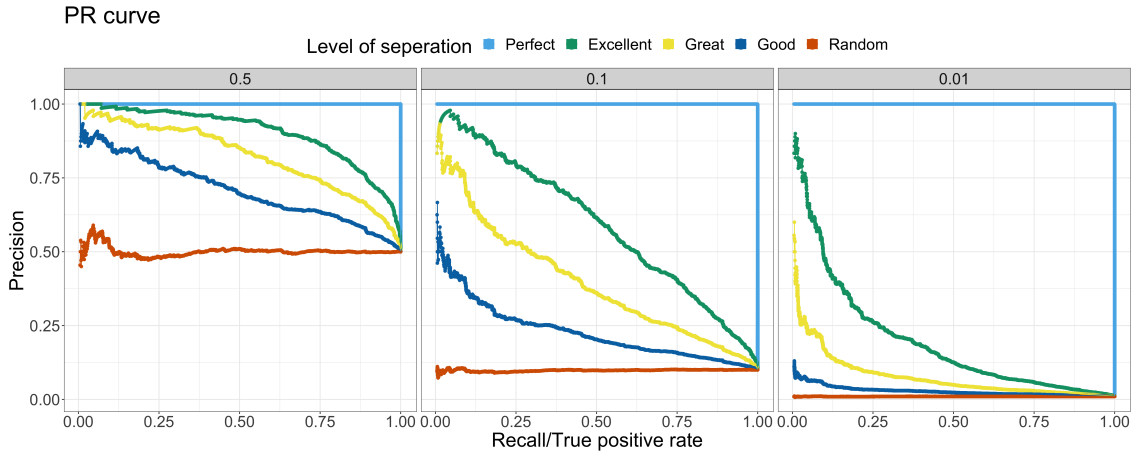

Figure 3.11: Examples of PR curves for the output of a binary classifier at various levels of separation and positive rates[5]

7 OBJECTIVE FUNCTIONS

We experimented with four different objective loss functions for handling biased data in Mesogeos and sparse segmentation.

7.1 BINARY CROSS-ENTROPY

Binary Cross-Entropy is a crucial metric in classification tasks, effectively capturing the difference between two probability distributions for a given random variable or event set. Widely adopted in classification objectives, particularly in segmentation tasks, which involve pixel-level classification, Binary Cross-Entropy is specifically tailored for scenarios where the target variable comprises two classes. This loss function evaluates the dissimilarity between the predicted probabilities and the true binary labels [47].

The Binary Cross-Entropy (BCE) loss is given by the formula:

$$\text{BCE}(y, \hat{y}) = -\frac{1}{N}\sum_{i=1}^{N}[y_i \log(\hat{y}_i) + (1 - y_i)\log(1 - \hat{y}_i) \tag{3.3}$$

Here, y represents the true label (either 0 or 1) for the given sample, while $\hat{y}$ denotes the predicted probability for the same sample belonging to Class 1, as determined by the prediction model.

7.2 WEIGHTED BINARY CROSS-ENTROPY

Weighted Binary Cross-Entropy (WCE) presents a modification of the standard binary cross-entropy approach. In WCE, positive examples receive weighting by a certain coefficient, making it particularly applicable in scenarios with imbalanced data distributions. This weighting adjustment aims to address the skewness in the data [47, 48]. It is defined as:

$$\text{WBCE}(y_{\text{true}}, y_{\text{pred}}, w_0, w_1) = -\left(w_1 \cdot y_{\text{true}} \cdot \log(y_{\text{pred}}) + w_0 \cdot (1 - y_{\text{true}}) \cdot \log(1 - y_{\text{pred}})\right) \tag{3.4}$$

where y_{true} represents the true label, y_{pred} signifies the predicted label, and w_0 and w_1 denote the weights assigned to negative and positive training data, respectively.

[5] Source: https://sinyi-chou.github.io/classification-pr-curve/

7.3 BINARY FOCAL CROSSENTROPY (BFCE)

Focal Binary Cross Entropy 3.5 is a loss function designed to address the challenge of extreme class imbalance in the training of one-stage object detectors. It modifies the standard cross-entropy loss by down-weighting well-classified examples, thereby focusing the training process on harder examples [47, 49].
The focal loss is mathematically expressed as: The Focal loss is defined as:

$$\text{FL}(p_t) = -\alpha_t(1-p_t)^{\gamma}\log(p_t) \tag{3.5}$$

where $\gamma > 0$ and α generally ranges from $[0, 1]$.

p_t represents the model's estimated probability for the true class, γ is a focusing parameter that controls the rate at which easy examples are down-weighted and α is a weight balancing factor that balances the importance of positive and negative examples during training, crucially addressing class imbalances. Typically set within the range [0, 1], α assigns weight to class 1, while $1-\alpha$ applies to class 0. The value of α can be based on inverse class frequency or set as a hyperparameter through cross-validation, effectively managing class imbalance and improving detection performance [49].

7.4 DICE COEFFICIENT-BINARY CROSSENTROPY

The Dice coefficient is a measure of overlap, generally employed in image segmentation tasks. [47, 50].The Dice coefficient loss is defined as:

$$\text{Dice\_Coef\_Loss}(y_{\text{true}}, y_{\text{pred}}) = 1 - \text{Dice\_Coef}(y_{\text{true}}, y_{\text{pred}}) \tag{3.6}$$

where y_{true} represents the true label, y_{pred} signifies the predicted label.
The Dice coefficient-Binary Crossentropy is a combination of Binary Crossentropy (Equation 3.3) and Dice coefficient loss (Equation 3.6). The Dice coefficient-Binary Crossentropy is defined as:

$$\text{BCE-Dice\_Loss}(y_{\text{true}}, y_{\text{pred}}) = \text{BCE}(y_{\text{true}}, y_{\text{pred}}) + \text{Dice\_Coef\_Loss}(y_{\text{true}}, y_{\text{pred}}) \tag{3.7}$$

The combination of Binary Cross Entropy (BCE) and Dice Loss is effective due to its ability to manage class imbalance. BCE helps optimize the network for binary classification tasks by measuring the difference between predicted and actual class probabilities. Dice Loss complements this by focusing on the spatial overlap between predicted and ground truth segmentation masks, enhancing the model's ability to capture fine details and boundaries. This balanced approach leverages the

strengths of both loss functions, leading to improved model performance and robustness [51].

8 EXPERIMENTAL DESIGN

Our experimentation was conducted primarily on Google Colab Pro, utilizing the resources provided by the Scientific Research Center of our university. Google Colab Pro offers access to powerful computing resources, including a T4 GPU with high RAM (approximately 50 GB of RAM), which proved essential role in alleviating resource limitations experienced on our local machines. To prevent overfitting and ensure optimal model performance, we implemented early stopping during training. This technique terminate the training process if the validation loss did not exhibit improvement over a specified number of epochs, thereby preventing the model from memorizing the training data and enhancing its generalization capability. Additionally, regularization techniques such as L2 regularization, dropout, and batch normalization were used.

To comprehensively evaluate the model's performance, we trained multiple instances of the models, each with a distinct combination of loss functions and learning rates using the Adam optimizer [52]. The loss functions included Binary Cross-Entropy, Focal Binary Cross-Entropy, Weighted Binary Cross-Entropy, and Dice_BCE Loss, while learning rates varied across three magnitudes: 10^{-3}, 10^{-4}, and 10^{-5}.

The models were evaluated using F1 Score, Dice Coefficient, and precision-recall (PR) curves to assess the models' performance.

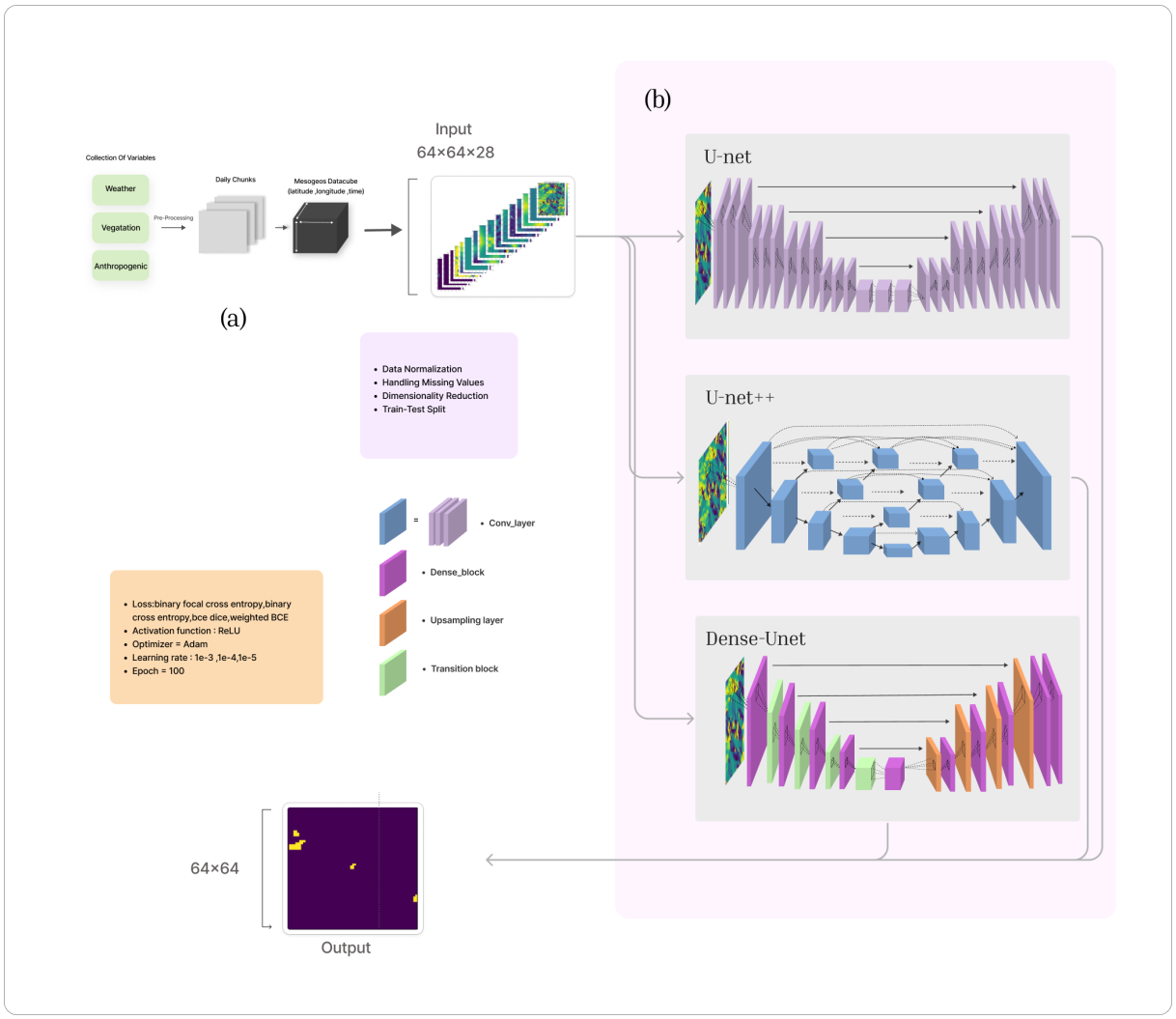

Figure 3.12: Deep Learning Methods used for Final Burned Area Prediction Using the mesogeos Data. (a): Mesogeos Data (b): Comparative Analysis of Unet, Unet++, and Dense-Unet Architectures, Including Dense-block (3.8), transition block (3.8)

9 RESULTS AND DISCUSSION

This section provides the key findings from previous studies and our experiments, offering a structured overview of the results obtained and their implications for the study objectives.

9.1 MESOGEOS RESULTS

The original authors of the dataset introduced the dataset and conducted an analysis to predict the likely extent of a wildfire's final burned area [3]. This task was formulated as a segmentation problem, where the goal was to estimate the probability of neighboring pixels around the ignition point being contained within the final burned area. The authors used a U-Net architecture with an EfficientNet-B1 encoder and evaluated the model using cross-entropy loss and AUPRC (The Precision-Recall curve) metrics.

In their experimental setup, they trained the models using data from 2006-2019, validated on 2020 data, and tested on 2021-2022 data. The model was trained in **a system with 2 GPUs (NVIDIA GeForce RTX 3090), each one having a memory of 24 GB**. The total RAM of the system is **128GB**, and it also has 32 CPUs.

The results showed that a model using all available variables slightly outperformed a baseline model that used only the ignition points. The reported performance metrics were:

Table 3.2: Results of the final burned area prediction task from previous study

Model	CE Loss	AUPRC
U-Net (only ignitions)	0.0177	0.394
U-Net (all variables)	0.0166	0.418

However, their approach left room for improvement in terms of accuracy, efficiency, or other relevant performance metrics.

9.2 U-NET RESULTS

Table 3.3 summarizes the performance of the U-Net model trained with different loss functions and learning rates.

Table 3.3: Performance of U-Net model with different loss functions and learning rates

Metric	BCE			FBBE			DICE_BCE			WBCE		
	10^{-3}	10^{-4}	10^{-5}	10^{-3}	10^{-4}	10^{-5}	10^{-3}	10^{-4}	10^{-5}	10^{-3}	10^{-4}	10^{-5}
Loss	0.03	0.02	0.03	0.04	0.01	0.02	0.72	1.27	1.20	0.02	0.02	0.22
F1 Score	0.36	**0.48**	0.35	0.30	0.36	0.31	**0.51**	0.30	0.33	0.23	0.23	0.22
Dice Coefficient	0,25	**0.35**	0.25	0.04	0.02	0.03	**0.50**	0.30	0.32	0.19	0.18	0.11
AUPRC	0.29	**0.46**	0.26	0.16	0.27	0.21	**0.42**	0.15	0.19	0.18	0.18	0.19

INTERPRETATION OF RESULTS(DISCUSSION)

In this section, The U-Net model's performance is evaluated under various loss functions and learning rates to predict wildfire burned areas, considering the challenging nature of our imbalanced dataset. The performance of the U-Net model, summarized in Table 3.3, shows that the model trained with Binary Cross-Entropy (BCE) loss and a learning rate of 10^{-4} and the model trained with Dice-BCE loss and a learning rate of 10^{-3} exhibited superior metrics compared to other configurations. the U-Net with BCE and 10^{-4} achieved F1 score(0.48), Dice coefficient (0.35), and AUPRC (0.46), while the U-Net with Dice-BCE and 10^{-3} showed the highest F1 score (0.51) and Dice coefficient (0.50) and a notable AUPRC (0.42). These results confirms that BCE is an effective loss function for such tasks, as it directly optimizes metrics related to pixel-wise classification. While the Focal Binary Cross-Entropy and Weighted Binary Cross-Entropy Loss are designed to address class imbalance in hard-to-classify examples, but their low losses and substandard performance in other metrics suggest they may not be sufficient for the complexity of the dataset. Dice-BCE combines the strengths of Dice loss and BCE, particularly suited for such tasks. The U-Net model with Dice-BCE loss with $\text{lr} = 10^{-3}$ demonstrated modest capabilities. The high F1 Score and Dice Coefficient indicate that Dice-BCE is more effective than BCE in capturing the extent of the burned area, providing detailed and accurate results. The visual predictions from the Dice-BCE model appear qualitatively better than those from the BCE. In comparing our U-Net model results with similar studies, it's evident that our approach, achieved performance metrics comparable to the original study, highlighting the complexity of the task. The study aimed to improve the U-Net model's accuracy in estimating final burned areas in wildfire scenarios, but found suboptimal performance despite experimenting with different configurations. The study suggests further refinement and investigation to improve the model's accuracy.

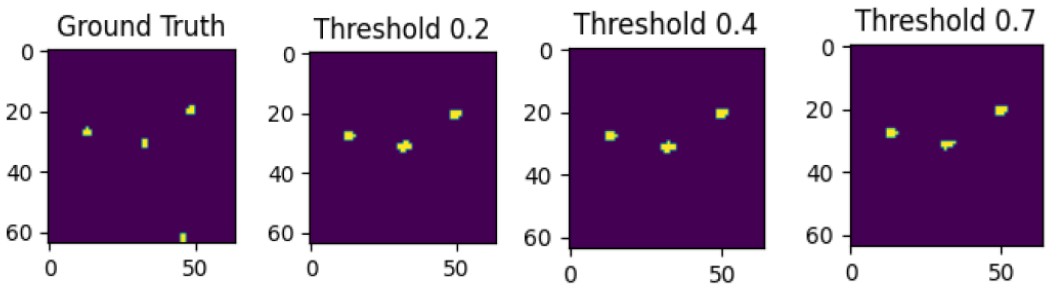

Figure 3.13: Unet prediction for Dice-BCE loss with lr $= 10^{-3}$

9.3 UNET++ RESULTS

We used U-Net++ due to the complex and imbalanced nature of dataset and the suboptimal performance of the UNet. U-net++ improvements provide richer context by integrating multi-scale features, which is particularly beneficial for addressing class imbalance and capturing fine details in complex datasets by ensure that encoder feature maps are semantically richer and better aligned with the decoder feature maps.

we applied the U-Net++ model to various loss functions, such as Binary Cross Entropy (BCE), Binary Focal CrossEntropy (BFC), Weighted Binary Cross Entropy (WBCE), a Dice Coefficient and Binary Cross Entropy combination (DICE-BCE) and different learning rates 10^{-3}, 10^{-4}, 10^{-5}. results as shown in the table 3.4.

Table 3.4: Performance of U-Net++ model with different loss functions and learning rates

Metric	BCE			FBBE			DICE_BCE			WBCE		
	10^{-3}	10^{-4}	10^{-5}	10^{-3}	10^{-4}	10^{-5}	10^{-3}	10^{-4}	10^{-5}	10^{-3}	10^{-4}	10^{-5}
Loss	0.01	0.02	0.024	0.0039	0.006	0.007	0.69	0.72	1.27	0.005	0.007	0.03
F1 Score	0.50	0.39	0.31	0.52	0.39	0.30	**0.52**	0.51	0.30	0.42	0.51	0 .27
Dice Coefficient	0.36	0.19	0.23	0.07	0.037	0.028	**0.52**	0.50	0.29	0.33	0.36	0.026
AUPRC	**0.49**	0.30	0.24	0.49	0.32	0.19	0.46	0.41	0.20	0.49	0.50	0.15

when combination the DICE and BCE, the best results are obtained with a learning rate $= 10^{-3}$ the most elevated F1 Score of 0.52 and Dice Coefficient of 0.52, and AUPRC of 0.46. The Binary Cross-Entropy (BCE) model performs well with a learning rate of 10^{-3}, achieving an F1 Score of 0.50, Dice Coefficient of 0.36, and AUPRC of 0.49. and The WBCE with a learning rate of 10^{-4}, achieving an F1 Score of 0.51 and AUPRC of 0.50, indicating its consistency in maintaining a good balance between false positives and false negatives. On the other hand, the Focal Binary Cross-Entropy (FBCE) model performs poorly at learning rates of 10^{-3}, 10^{-4}, 10^{-5} and WBCE in a

learning rate of 10^{-5} and BCE in a learning rate of 10^{-5}, and DICE-BCE in a learning rate of 10^{-5}. DICE-BCE loss is generally more efficient for U-Net++ in AUPRC, suggesting it provides a better balance of precision and recall.

while the results are good compared to U-Net, they are not sufficient for the performance required in wildfire segmentation tasks. This indicates a need for further performance improvements. Figure 3.14 below show prediction of U-Net++ model with DICE-BCE loss function and learning rates of 10^{-3}.

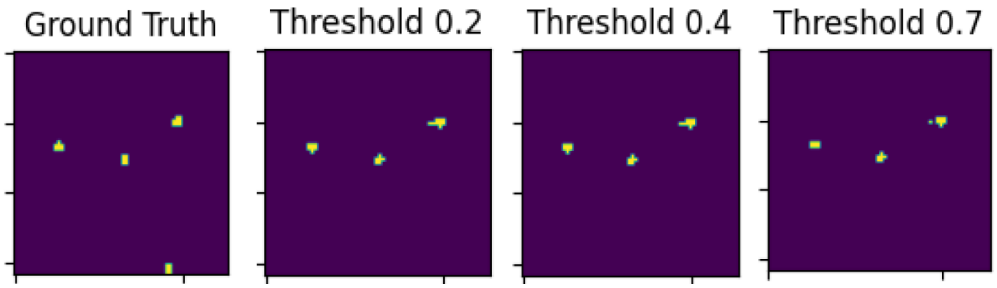

Figure 3.14: U-net++ prediction (DICE-BCE loss, lr = 10^{-3})

9.4 DENSE U-NET

Dense U-Net architecture, a variant of the U-Net model improved with dense connections. We used Dense U-Net because U-Net++ provided moderate results while increasing complexity. Dense U-Net, on the other hand, achieves comparable results with less complexity. we applied the Dense U-Net model to various loss functions, such as Binary Cross Entropy (BCE), Binary Focal CrossEntropy (BFC), Weighted Binary Cross Entropy (WBCE), a Dice Coefficient and Binary Cross Entropy combination (DICE-BCE) and different learning rates 10^{-3}, 10^{-4}, 10^{-5}. results as shown in the table 3.5.

Table 3.5: Performance of Dense U-Net model with different loss functions and learning rates

Metric	BCE			BFC			DICE_BCE			WBCE		
	10^{-3}	10^{-4}	10^{-5}	10^{-3}	10^{-4}	10^{-5}	10^{-3}	10^{-4}	10^{-5}	10^{-3}	10^{-4}	10^{-5}
Loss	0.01	0.01	0.01	0.003	0.004	0.005	0.67	0.70	1.10	0.005	0.008	0.009
F1 Score	0.49	0.48	0.43	0.50	0.51	0.45	**0.54**	0.52	0.35	0.42	0.49	0.44
Dice Coefficient	0.37	0.37	0.31	0.10	0.11	0.7	**0.54**	0.52	0.35	0.31	0.38	0.31
AUPRC	0.49	**0.50**	0.39	0.49	**0.50**	0.39	0.48	0.45	0.41	0.45	0.48	0.48

At a learning rate of 10^{-3}, the combination DICE-BCE got the greatest F1 Score (0.54) and Dice Coefficient (0.54) and AUPRC (0.48), demonstrating good segmentation and Precision recall balance. With a Dice Coefficient of (0.37) and AUPRC (0.49) and an F1 Score of 0.49, BCE at 10^{-3} also fared well. A learning rate of 10^{-4} yielded the best results for the BFC , AUPRC (0.50), which demonstrated modest performance across measures F1 Score of 0.51. The WBCE model remained consistent, with an F1 Score of 0.49, especially at10^{-4}. It was the most effective configuration compared to the other configuration, DICE-BCE at 10^{-3}.

Figure 3.15 below show prediction of Dense U-Net model with DICE-BCE loss function and learning rates of 10^{-3}.

Although the results are generally higher than those of U-Net++, they are still not sufficient to the segmentation task. indicating the need for further enhancements.

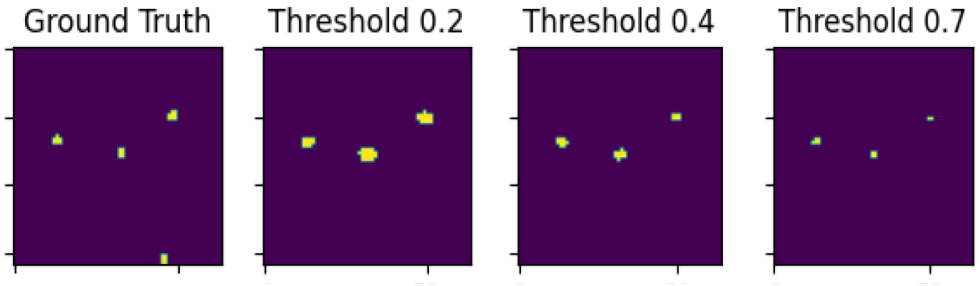

Figure 3.15: dense U net prediction (DICE-BCE loss , lr = 10^{-3})

10 COMPARATIVE ANALYSIS OF MODEL PERFORMANCES

in this section we compare the best results of the 3 models with the results of the original paper study.

Table 3.6: Performance Comparison of Different Architectures

model	F1 Score	Dice Coefficient	AUPRC
U-Net Original Paper	-	-	0.418
U-Net	0.51	0.50	0.42
U-Net++	0.52	0.52	0.46
Dense U-Net	0.54	0.54	0.48

Based on these results, the Dense U-Net model outperforms the other architectures in terms of

predictive capability, the superior performance of the Dense U-Net architecture makes it the most suitable choice to initiate further exploration and enhancement of wildfire prediction tasks.

11 CONCLUSION

In conclusion, this chapter provided a comprehensive overview of the data preparation, model architectures, objective functions, and evaluation metrics used in our research.

Finally, the discussion and results section presented a comparative study of the three models, analyzing their performance under different configurations of loss functions and learning rates. The findings provided valuable insights into each model, facilitating decision-making regarding model selection and optimization strategies.

Overall, this chapter served as a foundational component of our research, laying the groundwork for subsequent analyses and conclusions.

In the next chapter, we aim to develop robust and precise wildfire prediction models, ultimately enhancing wildfire management and mitigation strategies.

CHAPTER 4

CONTRIBUTION 2: INTEGRATING DENSE U-NET FOR WILDFIRE SEGMENTATION AND BURNED AREA ESTIMATION

1 INTRODUCTION

In this chapter, we introduce a novel approach that integrates the strengths of Dense U-Net to create a superior model for estimating the final burned area. We will assess the performance of this proposed architecture and compare it with results from other studies.

2 PROPOSED APPROACH

In this section, we introduce an approach that integrates size estimation as a regularization component to enhance wildfire segmentation using deep learning models. Traditional segmentation approaches often focus solely on delineating wildfire extents without considering the estimated size of the wildfire, leading to suboptimal results, especially in regions with varying wildfire sizes or complex spatial patterns.

Our proposed approach aims to address this limitation by leveraging size estimation as a regularization component within the segmentation task. The core idea behind our proposed approach is to optimize multiple objectives simultaneously during model training. By combining segmentation and size estimation objectives into a unified optimization framework, our approach enables the model to learn from both aspects of the data simultaneously, leading to improved segmentation quality.

In our proposed approach, we treat size estimation as a regularization term within the segmentation task. This regularization penalty encourages the segmentation model to produce predictions that are not only accurate in delineating wildfire extents but also aligned with the estimated sizes of the wildfires. By incorporating size-related information into the optimization process, we aim to refine the predicted boundaries of wildfire extents and improve segmentation accuracy.

Our approach involves jointly optimizing segmentation and size estimation objectives within the model architecture. By integrating size estimation, we ensure that both tasks contribute to the overall optimization process. This integrated approach allows the model to learn representations that effectively balance segmentation quality with size estimation accuracy.

2.1 OPTIMIZATION STRATEGY

During model training, our objective is to minimize both the segmentation loss and the regularization component loss associated with size estimation simultaneously. This dual optimization process encourages the model to produce segmentation masks that accurately delineate wildfire extents and

align with the estimated sizes of the wildfires. By penalizing deviations from the estimated sizes, the regularization term guides the segmentation process towards more consistent predictions.

The inclusion of a regularization component in the segmentation task is expected to yield advantages. Our approach improves segmentation accuracy in regions with varying wildfire sizes and complex spatial patterns, leveraging **additional information** for more reliable wildfire predictions.

Our proposed approach represents a novel method for enhancing wildfire segmentation using deep learning models. By integrating size estimation as a regularization technique within the segmentation task, we aim to improve segmentation quality and produce more accurate predictions of wildfire extents.

This approach offers a promising strategy for addressing the challenges associated with wildfire segmentation and advancing the state-of-the-art in this field.

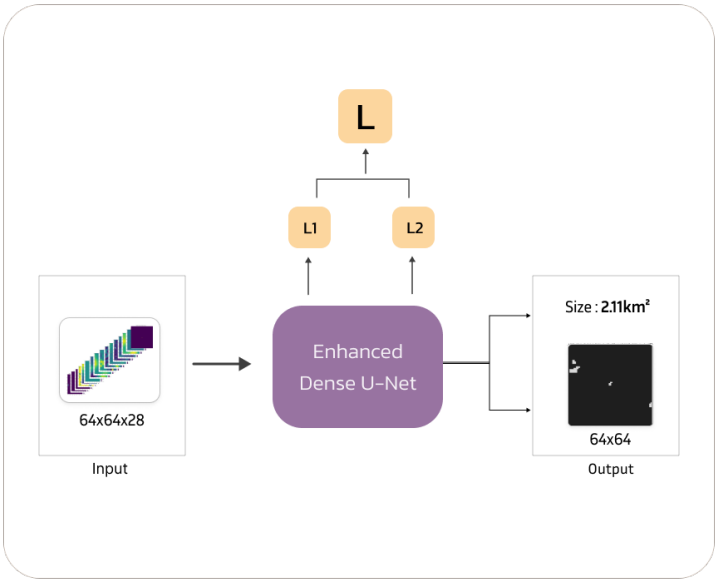

Figure 4.1: Enhanced Dense U-Net for Prediction burend area and estimating wildfire sizes

3 IMPLEMENTATION

In our research, we compared the performance of three models: U-Net++, U-Net, and Dense U-Net. The results showed that Dense U-Net outperformed the other models. For segmenting burned areas, we used a Dense U-Net model. Dense U-Net is created using dense blocks and transition layers. Dense blocks contain convolutional layers with batch normalization, ReLU, and dropout. Then, We

use dense layers to estimate the size of the burned areas. We chose the Dense U-Net architecture because it works well in tasks that involve segmenting areas, especially when capturing fine details is important.

The Adam optimizer is utilized, with a learning rate set to 0.01. Early stopping and L2 regularization were employed to prevent overfitting and improve convergence during training. The loss function combines the mean squared error [53] for prediction size with the DICE-BCE loss for segmentation. Performance is assessed using customized measures such as R-squared [53], balanced accuracy 3.1, and the F1 score. The significance of the segmentation and prediction size is balanced by adjusting the loss weights.

3.1 BALANCED ACCURACY

Balanced accuracy is a performance metric used in binary and multi-class classification tasks, particularly in imbalanced datasets. It considers both sensitivity (recall) and specificity [54]. The balanced accuracy is defined as:

$$\text{Balanced Accuracy} = \frac{\text{Sensitivity} + \text{Specificity}}{2} \tag{4.1}$$

Where:

Sensitivity (or recall) measures the proportion of actual positives that are correctly identified:

$$\text{Sensitivity} = \frac{TP}{TP + FN} \tag{4.2}$$

Specificity measures the proportion of actual negatives that are correctly identified:

$$\text{Specificity} = \frac{TN}{TN + FP} \tag{4.3}$$

4 RESULTS AND DISCUSSION

Table 4.1 summarizes the performance of Proposed Model trained. The model's performance was evaluated using Loss, F1 Score, Dice Coefficient, Balanced Accuracy, and AUPRC metrics.

Table 4.1: Performance metrics of the enhanced Dense U-net

Model	F1 Score	Dice Coefficient	Balanced Accuracy	AUPRC
enhanced Dense U-Net	0.57	0.55	0.77	0.54

The proposed Dense U-Net model achieved a Loss of 0.48, an F1 Score of 0.57, a Dice Coefficient of 0.55, a Balanced Accuracy of 0.77, and an AUPRC of 0.54. These metrics indicate that the model is performing well in both segmentation and size estimation tasks. Both F1 Score and Dice Coefficient metrics are relatively high, with values of 0.57 and 0.55, respectively. These scores reflect the model's precision and recall, confirming its competence in distinguishing between burned and unburned areas. With a balanced accuracy of 0.77, the model demonstrates a good balance between sensitivity and specificity. This is particularly important in wildfire segmentation, where both false positives and false negatives can have significant importance. The AUPRC scores of 0.54 as shown in 4.3, shows that the model performs well in terms of precision-recall trade-offs, which is crucial in our extremely imbalanced data.

The figure below shows some predictions the enhanced Dense U-net.

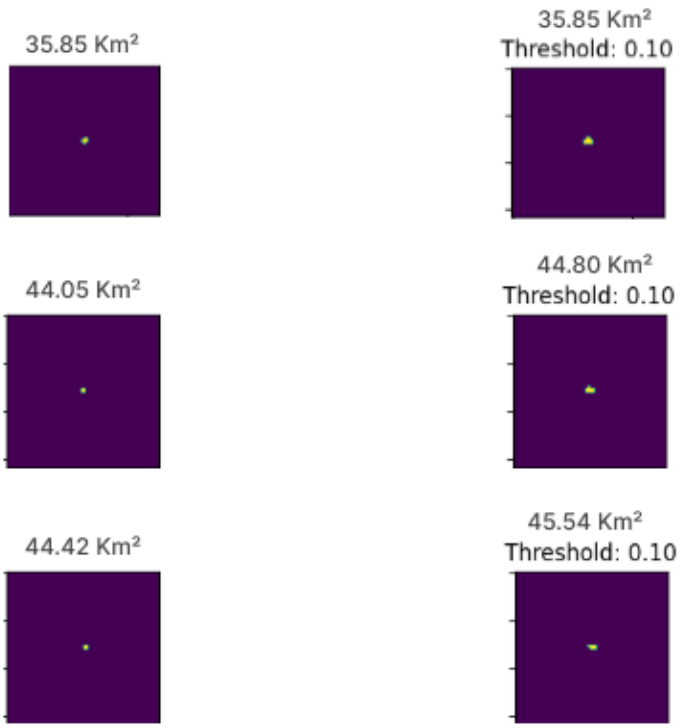

Figure 4.2: Predictions using the enhanced Dense U-net architecture

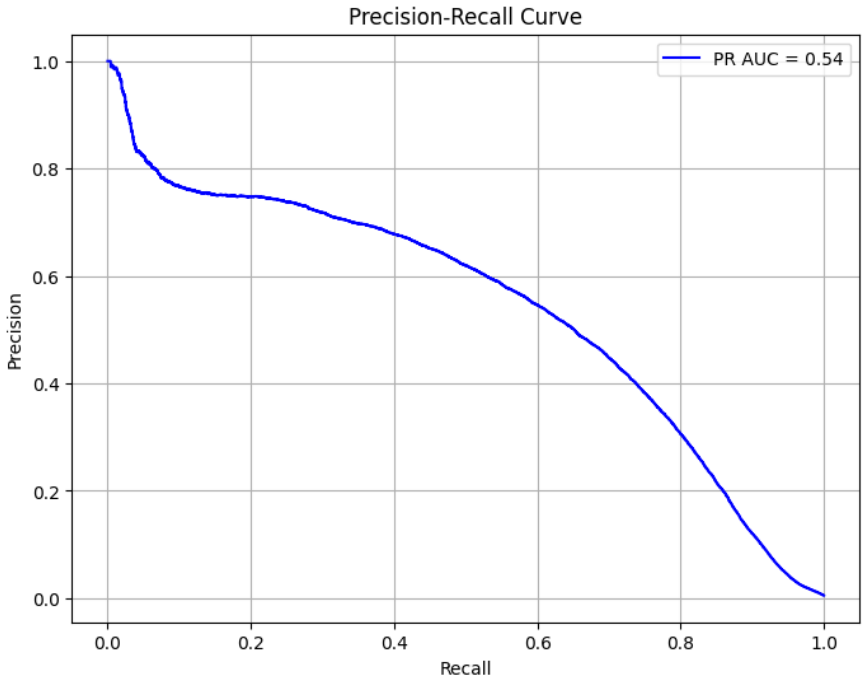

Figure 4.3: AUPRC of the the Enhanced Dense U-net

4.1 COMPARATIVE ANALYSIS OF MODEL PERFORMANCES

we compared the best results of the 3 models with the results of the dense unet enhanced in term of F1 Score and AUPRC.

Table 4.2: Comparison of Performance Metrics for Different Architectures

Architecture	F1 Score	AUPRC
U-Net Original Paper	-	0.418
U-Net	0.51	0.42
U-Net++	0.52	0.46
Dense U-Net	0.54	0.48
Enhanced Dense U-net	0.57	0.54

The comparative analysis reveals the superiority of our enhanced Dense U-Net model over other U-Net architectures. Compared to the original U-Net paper, our model shows a significant improvement in AUPRC. Additionally, when compared to U-Net, U-Net++, and basic Dense U-Net, our modified Dense U-Net model achieves notably higher scores in both metrics. Overall, our proposed

enhanced Dense U-Net model shows notable improvements over other models, providing a more reliable and accurate method for wildfire segmentation and burned area estimation. The integration of size estimation as a regularization component has proven to be beneficial, leading to enhanced model performance across various metrics.

5 CONCLUSION

In conclusion, this chapter introduced an innovative approach that integrates Dense U-Net architecture for wildfire segmentation and burned area size estimation. Our approach outperforms other U-Net architectures, offering superior performance in wildfire management and risk assessment through more accurate delineation of burned areas.

Furthermore, in the next chapter, we will explore another approach to further enhance our predictions.

CHAPTER 5

CONTRIBUTION 3:DENOISING DENSE U-NET

1 INTRODUCTION

In this chapter, we present a new architecture for predicting the final burned area by enhancing the Dense U-Net model. Our approach aims to improve the accuracy and reliability of wildfire segmentation and burned area estimation. We evaluate the performance of this architecture and compare it with previous models.

2 DENOISING DENSE U-NET

The proposed model architecture is a combination of two networks: a segmentation network and a refinement network.

2.1 SEGMENTATION MODULE: SEGMENTATION NETWORK

The segmentation network used is a Dense U-Net, chosen for its balance of prediction accuracy and computational complexity.

The network's objective is to perform initial segmentation predictions. The input shape of the model is (64, 64, 28), representing 64x64 pixels with 28 channels corresponding to the input features or image modalities. The output of the segmentation network is subsequently used as input for the refinement network.

2.2 REFINEMENT MODULE: REFINEMENT NETWORK

The module includes a refinement network serves as a denoising module to improve the segmentation masks produced by the initial segmentation network.

This network employs an auto-encoder architecture with attention mechanisms [55] justified by its ability to focus on crucial features and regions, which helps in refining the segmentation outputs.

The input to this network is the segmentation masks generated by Segmentation Network. By iteratively refining the segmentation masks, the module improves segmentation accuracy and boundary delineation.

3 TRAINING PROCEDURE

The model is trained using the Adam optimizer with a learning rate of 1e-3. The loss function employed is BCE-Dice loss. The training process involves minimizing the combined loss of the segmentation and refinement outputs, focusing on optimizing the segmentation performance while leveraging the refinement network to enhance segmentation quality. Each network's loss is calculated separately, providing deep supervision and allowing for coordinated optimization of parameters. This integrated training approach enables the model to optimize parameters in a coordinated manner to enhance performance and computational efficiency.

Early stopping is employed to prevent overfitting and improve convergence during training. the Performance metrics used during training and evaluation are balanced accuracy, F1 score, Dice Coefficient, and the area under the precision-recall curve (AUPRC).

Figure 5.1 below shows the Denoising Dense U-Net architecture.

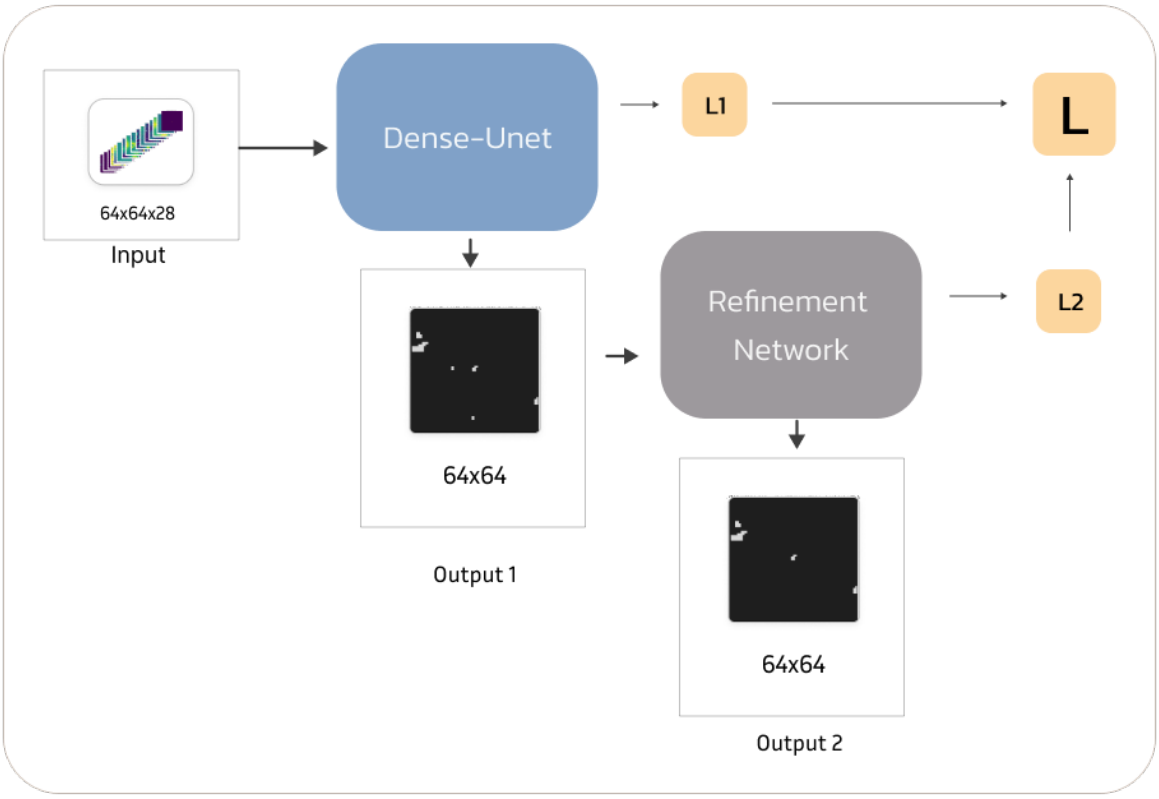

Figure 5.1: Architecture of the proposed Denoising Dense U-Net

4 RESULTS AND DISCUSSION

The results presented in Table 5.1 highlight the performance metrics achieved by the proposed Denoising Dense U-Net.

Table 5.1: Performance metrics of the Denoising Dense U-Net

Model	F1 Score	Dice Coefficient	Balanced Accuracy	AUPRC
Segmentation Module	0.56	0.55	0.77	0.52
Refinement Module	0.57	0.56	0.78	0.54

The results show significant improvements with the addition of the Refinement Module to the Dense U-Net architecture.

The Segmentation Module achieved an F1 score of 0.56, which increased to 0.57 with the Refinement Module, indicating enhanced precision and recall balance. Similarly, the Dice Coefficient improved from 0.55 to 0.56 with the addition of the Refinement Module, demonstrating more accurate segmentation outcomes. Balanced Accuracy for the Segmentation Module was 0.77, while the Refinement Module improved this metric to 0.78, reflecting superior classification performance across different classes. Additionally, the Area Under the Precision-Recall Curve (AUPRC)as shown in 5.3 increased from 0.52 to 0.54 with the Refinement Module.

The use of an auto-encoder architecture with attention mechanisms plays a crucial role in this improvement. By focusing on critical areas and iteratively refining the segmentation outputs, the model achieves more precise and reliable segmentation results. This approach is particularly effective in complex regions where accurate boundary delineation is challenging.

The figure below shows some predictions the Denoising Dense U-Net.

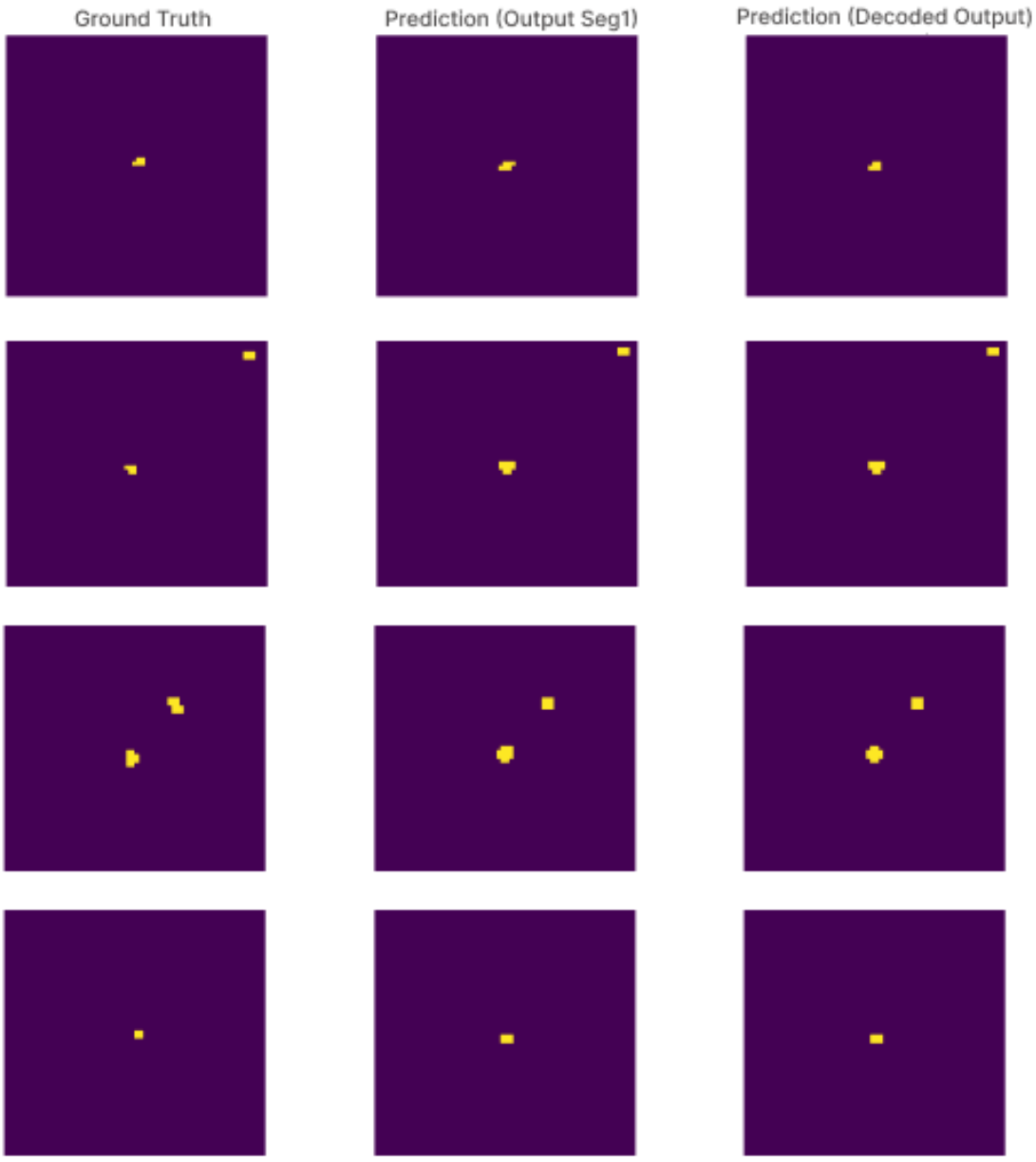

Figure 5.2: Predictions of the Denoising Dense U-Net: ground truth vs Segmentation module output vs Final Denoising Dense U-Net output

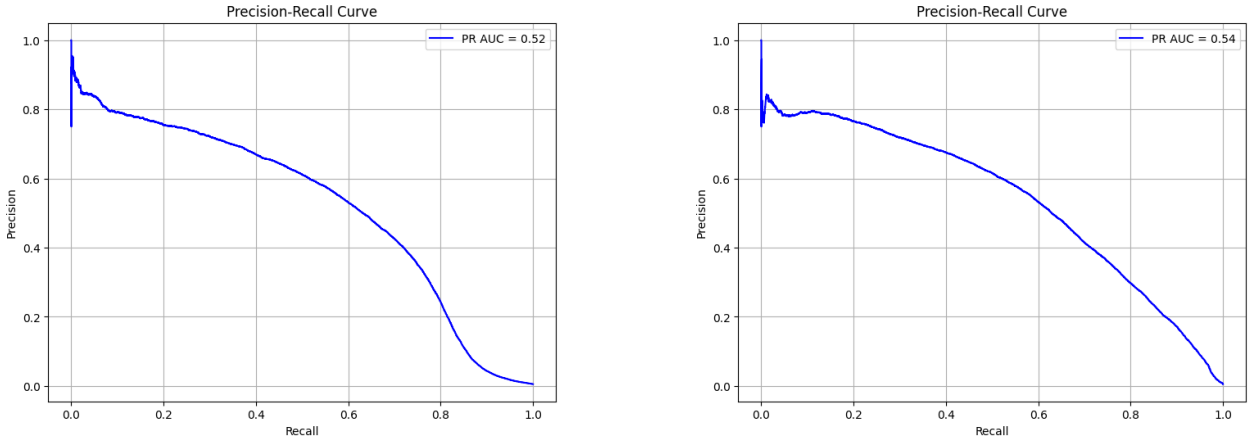

(a) AUPRC of the segmentation module

(b) AUPRC of the Denoising Dense U-Net

Figure 5.3: AUPRC for our Model

4.1 COMPARATIVE ANALYSIS OF MODEL PERFORMANCES

we compared the best results of the 3 models with the results of the Denoising Dense U-Net in term of F1 Score and AUPRC.

Table 5.2: Performance Comparison of Different Architectures

Architecture	F1 Score	AUPRC
U-Net Original Paper	-	0.418
U-Net	0.51	0.42
U-Net++	0.52	0.46
Dense U-Net	0.54	0.48
Enhanced Dense U-net	0.57	0.54
Denoising Dense U-Net	0.57	0.54

The comparative analysis highlights the performance improvements of various models in terms of F1 Score and AUPRC. Traditional models like U-Net variants and Dense U-Net showed substandard performance. Our Enhanced Dense U-Net and Denoising Dense U-Net models surpassed the others, with similar performance metrics but differing in complexity, with the enhanced Dense Unet having 9,446,427 trainable parameters and the Denoising Dense U-Net having 16,665,074 trainable parameters. achieving an AUPRC of 0.54 and an F1 Score of 0.57.

These results underscore the efficacy of the refinement strategy in enhancing segmentation

accuracy and burned area estimation. These results validate the proposed architecture's potential to advance the state-of-the-art in wildfire segmentation, offering valuable insights for future research and practical applications in wildfire management.

Overall, the proposed Denoising Dense U-Net model demonstrates substantial improvements over the basic Dense U-Net, providing a more accurate method for wildfire segmentation and burned area estimation. However, a significant limitation of our proposed models is inherently linked to the characteristics of our dataset.

5 CONCLUSION

In this chapter, we prposed a new architecture for predicting the final burned area using the Dense U-Net model. Our approach aims to enhance the accurate of wildfire segmentation and burned area estimation. The proposed Denoising Dense U-Net model consists of a segmentation network and a refinement network, which especially enhances segmentation performance by iteratively refining segmentation masks. This refinement process is conducted through an auto-encoder architecture with attention mechanisms, Our proposed model outperforms other U-Net architectures such as U-net, U-net++, and Dense Unet.

General Conclusion

In conclusion, our thesis aimed to enhance wildfire management by developing advanced approaches to predict the extent of wildfire damage. We used cutting-edge deep learning methods, specifically the U-net variants, for accurate wildfire final burned area prediction and estimation.

In the first chapter, we explored the various challenges in wildfire prediction and management, emphasizing the need to consider external factors such as weather conditions, vegetation characteristics, and human activities. We discussed how wildfires profoundly impact ecosystems, human health, and the economy. Additionally, we reviewed current applications of machine learning and deep learning in wildfire prediction and management.

In the second chapter, we reviewed the literature and existing methodologies for wildfire extent prediction. We identified the limitations of current models, such as neglecting important external factors and lacking generalizability across different regions. This chapter sets the foundation for our proposed methods by outlining the key gaps in current research.

In the third chapter, we focused on a comparative study of three different models: U-net, U-net++, and Dense U-net in wildfire final burned area prediction, addressing the significant dataset imbalance evaluated using the Mesogeos dataset and aiming to identify the most effective architecture for wildfire prediction. Our analysis revealed that the Dense U-net model outperformed the others, demonstrating superior predictive capabilities.

In the fourth chapter, we introduced a novel approach integrating Dense U-net for wildfire segmentation and burned area estimation. This approach combined segmentation and size estimation into a unified optimization framework, resulting in improved accuracy and reliability of wildfire predictions.

In the fifth chapter, we presented an advanced architecture. This model designed to further enhance prediction accuracy and reliability. Through evaluations, our architecture demonstrated

significant improvements over previous U-net variant models, achieving similar performance as the enhanced dense U-net mentioned in the previous chapter, marking a substantial contribution to wildfire prediction methodologies.

According to experiments, the approaches we proposed showed promising results. as they outperformed other methods we compared with them. Future work will consider further analysis and enhancements of the proposed models by incorporating 3D convolutional neural networks. Moreover, a deeper study of the dataset, including a more detailed analysis of various features, could provide valuable insights to improve prediction accuracy, leading to significant improvements in wildfire management and risk assessment.

BIBLIOGRAPHY

[1] K. Stavros, C. Fotios, K. Dimitrios, P. Christina, and P. Aristidis, "Socio-psychological, economic and environmental effects of forest fires," *Fire*, vol. 6, no. 7, 2023.

[2] M. Pandey, A. Arora, M. Siddiqui, S. Mitra, N. Pandey, S. Soni, A. Kaur, and U. Shukla, "Linkage between the forest fires and the meteorological parameters during the current climatic regime using spatial clustering, regression, and combination matrix analysis," *EarthArXiv*, 02 2021.

[3] S. K. I. P. G. Camps-Valls2 and I. Papoutsis1, "Mesogeos: A multi-purpose dataset for data-driven wildfire modeling in the mediterranean," *https://arxiv.org/pdf/2306.05144*, 2023.

[4] O. Ronneberger, P.Fischer, and T. Brox, *U-Net: Convolutional Networks for Biomedical Image Segmentation*, vol. 9351 of *LNCS*. Springer, 2015. (available on arXiv:1505.04597 [cs.CV]).

[5] Z. Zhou, M. M. R. Siddiquee, N. Tajbakhsh, and J. Liang, "Unet++: A Nested U-Net Architecture for Medical Image Segmentation," *arXiv: Computer Vision and Pattern Recognition*, jul 18 2018.

[6] S. Cai, Y. Tian, H. Lui, H. Zeng, Y. Wu, and G. Chen, "Dense-unet: a novel multiphoton in vivo cellular image segmentation model based on a convolutional neural network," *Quantitative Imaging in Medicine and Surgery*, vol. 10, pp. 1275–1285, 2020.

[7] N. G. Society, "Wildfires."

[8] K. Wolfgang, G. Matteo, M. Marco, B. Margherita, P. Gilberto, H. Wanqin, S. Sara, and P. Christopher, "Gis and machine learning for analysing influencing factors of bushfires using 40-year spatio-temporal bushfire data," *ISPRS*, 2022.

[9] S. K. I. P. I. P. N. Carvalhais, "Wildfire danger prediction and understanding with deep learning," *Geophysical Research Letters*, p. 1, 2022.

[10] A. M. I. G. T. F. A. G. I. Pires, "The hell of wildfires: The impact on wildlife and its conservation and the role of the veterinarian," *Conservation2023*, no. 3, pp. 96–108, 2023.

[11] M. Grillakis and A. Voulgarakis, "Hydrological impacts of wildfires at a global scale." Available at: https://doi.org/10.5194/egusphere-egu23-11112, 2023. Accessed: April 30, 2024.

[12] R. Z. L. B. Maribel Casas Vikas Kumar Linn Moore Andre Oliveira and A. Hicks, "Impacts of wildfire smoke and air pollution on a pediatric population with asthma: A population-based study," *International Journal of Environmental Research and Public Health*, vol. 20, no. 1937, 2023.

[13] B. M. S. K. E. H. B. G. L. N. R. E, "Deep learning approach to improve spatial resolution of goes-17 wildfire boundaries using viirs satellite data," *remote sensing*, vol. 16, no. 715, 2024.

[14] J. E. K. Juli G. Pausas, "A burning story: The role of fire in the history of life," *BioScience*, 2009.

[15] W. A. P., A. J. T., G. A., G.-M. J., B. D. A., J. K. Balch, and D. P. Lettenmaier, "Observed impacts of anthropogenic climate change on wildfire in california," *Earth's Future*, vol. 7, pp. 892–910, 2019.

[16] M. E. d. M. H. B. L. M. B. M. H. L. D. L. Susana Burrya Patricia I. Palaciob Mariano Somozaa, "Dynamics of fire, precipitation, vegetation and ndvi in dry forest environments in nw argentina. contributions to environmental archaeology," *Journal of Archaeological Science*, 2017.

[17] C. T. B. J. S. X. C. M. D. Flannigan, "Wildfire management in canada: Review, challenges and opportunities," *Progress in Disaster Science*, 2019.

[18] M. J. J. M. O. K. A. K. S. Shelke, "Forest wildfire detection using deep learning," *International Journal for Research in Applied Science Engineering Technology (IJRA)*, vol. 11, pp. 4951–4954, 2023.

[19] P. A. Prajith A M, "Forest wildfire detection from satellite images using deep learning," *International Journal of Advanced Research in Science, Communication and Technology (IJARSCT)*, vol. 3, pp. 578–583, 2023.

[20] B. P. C. A. M. G. P. V. R. M. S. M. V. G. A, "Cyber-physical system for wildfire detection and firefighting," *Future Internet*, vol. 15, 2023.

[21] P. J. S. C. S. S. M. C. S. T. M. Flannigan, "A review of machine learning applications in wildfire science and management," *Environmental Reviews*, 2020.

[22] A. M. Paulo Cortez, "A data mining approach to predict forest firesusing meteorological data," *Journal not found*, 2007.

[23] K. M. Guruh Fajar Shidik, "A data mining approach to predict forest firesusing meteorological data," *Lecture Notes in Computer Science*, vol. 8407, 2014.

[24] S. R. C. C. A. G. Y. C. P. S. E. Foufoula-Georgiou and J. T. Randerson, "Machine learning to predict final fire size at the time of ignition," *International Journal of Wildland Fire*, vol. 28, p. 861–873, 2019.

[25] K. Gökkaya, "Burned area and fire severity prediction of a forest fire using a sentinel 2-derived spectral index in Çanakkale, turkey," *Turkish journal of bioscience and collections*, vol. 6, no. 2, pp. 37–44, 2022.

[26] I. K. Lee, J. C. Trinder, and A. Sowmya, "Application OF U-NET CONVOLUTIONAL NEURAL NETWORK TO BUSHFIRE MONITORING IN AUSTRALIA WITH SENTINEL-1/-2 DATA," *The International Archives of the Photogrammetry, Remote Sensing and Spatial Information Sciences*, vol. XLIII-B1-2020, pp. 573–578, aug 6 2020.

[27] A. Y. Cho, P. S. E, K. D. J, K. J, L. C, and S. J, "Burned Area Mapping Using Unitemporal PlanetScope Imagery With a Deep Learning Based Approach," *IEEE Journal of Selected Topics in Applied Earth Observations and Remote Sensing*, vol. 16, pp. 242–253, 2023.

[28] F. A, C. L, and G. P, "Double-Step U-Net: A Deep Learning-Based Approach for the Estimation of Wildfire Damage Severity through Sentinel-2 Satellite Data," *Applied Sciences*, vol. 10, p. 4332, jun 24 2020.

[29] Y. W. SingChun Wang, "Predicting wildfire burned area in south central us using integrated machine learning techniques," *Atmospheric Chemistry and Physics*, no. 25, 2019.

[30] X. Hu, Y. Ban, and A. Nascetti, "Uni-Temporal Multispectral Imagery for Burned Area Mapping with Deep Learning," *Remote Sensing*, vol. 13, p. 1509, apr 14 2021.

[31] R. B. A MuUDWg EDROX, "Estimation of the burned area in forest fires using computational intelligence techniques," *Scientific reports*, vol. 11, no. 1, p. 6, 2012.

[32] Y. E. S. G. de Oliveira Gabriel Pereira Egidio Arai Francielle Cardozo Andeise Cerqueira Dutra Guilherme Mataveli, "Assessment of burned areas during the pantanal fire crisis in 2020 using sentinel-2 images," *Fire*, p. 14, 2023.

[33] H. Luft, C. Schillaci, G. Ceccherini, D. Vieira, and A. Lipani, "Deep learning based burnt area mapping using sentinel 1 for the santa cruz mountains lightning complex (czu) and creek fires 2020," *Fire*, vol. 5, no. 5, pp. 163–163, 2022.

[34] S. R. Coffield, C. A. Graff, Y. Chen, P. Smyth, E. Foufoula-Georgiou, and J. T. Randerson, "Machine learning to predict final fire size at the time of ignition," *International Journal of Wildland Fire*, vol. 28, no. 11, pp. 861–873, 2019.

[35] L. Knopp, M. Wieland, M. Rättich, and S. Martinis, "A Deep Learning Approach for Burned Area Segmentation with Sentinel-2 Data," *Remote Sensing*, vol. 2422, 2020.

[36] A. K. Brand and A. Manandhar, "Semantic segmentation of burned areas in satellite images using a u-net-based convolutional neural network," *The International Archives of the Photogrammetry, Remote Sensing and Spatial Information Sciences*, pp. 47–53, 2021.

[37] J. A. S. Remah Younisse, Rawan Ghnemat, "Fine-tuning U-net for medical image segmentation based on activation function, optimizer and pooling layer," *International Journal of Electrical and Computer Engineering (IJECE)*, vol. 13, p. 5406, oct 1 2023.

[38] C. Williams, F. Falck, G. Deligiannidis, C. C. Holmes, A. Doucet, and S. Syed, "A unified framework for u-net design and analysis," *Advances in Neural Information Processing Systems*, 2023.

[39] M. U. Rehman, S. Cho, J. H. Kim, and K. T. Chong, "Bu-Net: Brain Tumor Segmentation Using Modified U-Net Architecture," *Electronics*, vol. 9, p. 2203, dec 21 2020.

[40] M. D. Alahmadi, "Multiscale attention u-net for skin lesion segmentation," *IEEE Access*, vol. 10, pp. 59145–59154, 2022.

[41] V. Iglovikov and A. Shvets, "Ternausnet: U-Net with VGG11 Encoder Pre-Trained on ImageNet for Image Segmentation." https://arxiv.org/abs/1801.05746, jan 17 2018.

[42] N. Siddique, P. Sidike, C. Elkin, and V. Devabhaktuni, "U-Net and its variants for medical image segmentation: theory and applications," *IEEE Access*, vol. 9, pp. 82031–82057, nov 2 2021.

[43] Y. Cao, S. Liu, Y. Peng, and J. Li, "Denseunet: densely connected unet for electron microscopy image segmentation," *IET Image Processing*, vol. 14, pp. 2682–2689, 2020.

[44] A. Tharwat, "Classification assessment methods," *Applied Computing and Informatics*, 2020.

[45] R. R. Shamir, Y. Duchin, J. Kim, G. Sapiro, and N. Harel, "Continuous dice coefficient: a method for evaluating probabilistic segmentations.," *arXiv: Computer Vision and Pattern Recognition*, 2019.

[46] C. Williams, "The effect of class imbalance on precision-recall curves," *Neural Computation*, vol. 33, no. 4, pp. 853–857, 2021.

[47] S. Jadon, "A survey of loss functions for semantic segmentation," *2020 IEEE Conference on Computational Intelligence in Bioinformatics and Computational Biology (CIBCB)*, pp. 1–7, 2020.

[48] N. Bhatia, D. Mahesh, J. Singh, and M. Suri, "Bird-area water-bodies dataset (bawd) and predictive ai model for avian botulism outbreak (avi-bot).," *arXiv: Quantitative Methods*, 2021.

[49] T.-Y. Lin, P. Goyal, R. Girshick, K. He, and P. Dollár, "Focal loss for dense object detection," *IEEE Transactions on Pattern Analysis and Machine Intelligence*, vol. 42, no. 2, pp. 318–327, 2020.

[50] A. Carass, S. Roy, A. Gherman, J. Reinhold, A. Jesson, T. Arbel, O. Maier, H. Handels, M. Ghafoorian, B. Platel, A. Birenbaum, H. Greenspan, D. Pham, C. Crainiceanu, P. Calabresi, J. Prince, W. Roncal, R. Shinohara, and I. Oguz, "evaluating white matter lesion segmentations with refined sørensen-dice analysis," *Scientific Reports*, vol. 10, 2020.

[51] V. Rajput, "Robustness of different loss functions and their impact on networks learning capability," *ArXiv*, vol. abs/2110.08322, 2021.

[52] D. P. Kingma and J. Ba, "Adam: A method for stochastic optimization," *CoRR*, 2015.

[53] D. Chicco, M. J. Warrens, and G. Jurman, "The coefficient of determination r-squared is more informative than smape, mae, mape, mse and rmse in regression analysis evaluation," *PeerJ Computer Science*, vol. 7, p. 623, 2021.

[54] K. H. Brodersen, C. S. Ong, K. E. Stephan, and J. M. Buhmann, "The balanced accuracy and its posterior distribution," pp. 3121–3124, 2010.

[55] O. Oktay, J. Schlemper, L. L. Folgoc, M. J. Lee, M. P. Heinrich, K. Misawa, K. Mori, S. G. McDonagh, N. Y. Hammerla, B. Kainz, B. Glocker, and D. Rueckert, "Attention u-net: Learning where to look for the pancreas," *ArXiv*, vol. abs/1804.03999, 2018.